Volume 1 | Number 1 | Jan 2013 | Pages 1–100
NJC
New Journal of Chemistry
A journal for new directions in chemistry

Experimental and computational insights into the nature of weak intermolecular interactions in trifluoromethyl substituted isomeric crystalline *N*-methyl-*N*-phenylbenzamides.

Piyush Panini[a], *Deepak Chopra*[a*]

[a] *Crystallography and Crystal Chemistry Laboratory, Department of Chemistry, Indian Institute of Science Education and Research Bhopal, Madhya Pradesh, India-462066. Fax: 91-0755-6692392. Email: dchopra@iiserb.ac.in*

Abstract

The knowledge about the prevalence of weak interactions in terms of the nature and energetics associated with their formation is of significance in organic solids. In the current manuscript, we have systematically explored the existence of different types of intermolecular interactions in ten out of the fifteen newly synthesized trifluoromethyl derivatives of isomeric N-methyl-N-phenylbenzamides. The detailed analysis of all the crystalline solids were performed with quantitative inputs from interaction energy calculations using the PIXEL method. These studies revealed that in the absence of a strong hydrogen bond, the crystal packing is mainly stabilized by a co-operative interplay of weak C-H···O=C, C-H···π, C(sp^2)/(sp^3)-H···F-C(sp^3) hydrogen bonds along with other related interactions, namely π···π and C(sp^3)-F···F-C(sp^3). It is of interest to observe the presence of short and directional weak C-H···O=C hydrogen bonds in the packing, having a substantial electrostatic (coulombic + polarization) contribution towards the total stabilization energy. The C(sp^3)-F group were recognized in the formation of different molecular motifs in the crystal packing utilizing different intermolecular interactions. The contribution from electrostatics amongst the different weak hydrogen bonds was observed in decreasing order: C-H···O=C > C-H···F-C(sp^3) > C-H···π. Furthermore, there is an increase in the electrostatic component with concomitant decrease in the dispersion component for the shorter and directional hydrogen bonds.

Introduction

The study of intermolecular interactions, which links the molecules in the solid state, has been crucial and of prime focus in the area of crystal engineering [1-6]. In this regard, strong hydrogen bonds (e.g N/O-H···N/O) along with weak hydrogen bonds (like C-H···O/N/C) have been now well understood and recognized in the area of chemistry and biology [7-11]. The recent emphasis in the area of crystal engineering is on the understanding of weak intermolecular interactions, particularly those involving organic fluorine [12-13]. The replacement of hydrogen with fluorine atom was recognized to affect the physicochemical properties of a compound without much change in the molecular size [14-15]. It shows greater increase in stability which results in the increased resistance of a compound towards metabolic degradation [16-17]. There are 20% of pharmaceuticals and 30% of agrochemicals which were reported to possess organic fluorine and this number is still increasing [18]. The participation of organic fluorine in the participation of different intermolecular interactions was initially questioned amongst the researchers [19]. In the last decade, many studies on the participation of organic fluorine in different intermolecular interactions have been studied and their role in the formation of different supramolecular arrangements has been recognized [20-25]. The significance of these interactions has been very well summarized in a recent review [26], perspective [27] and a highlight [28]. The significance of such weak intermolecular interactions involving organic fluorine were studied both in the presence and absence of strong hydrogen bonds [29-35]. The missing link in these was the systematic study of these interactions in terms of the electronic nature of the participating fluorine atoms *i.e* fluorine atom connected to the C-atom of a different state of hybridization. Most of the past investigations involved the presence of a fluorine atom present on the phenyl ring (C-atom in sp^2 hybridized state). We have recently investigated the capability of fluorine atom connected to an sp^3 hybridized C-atom in the trifluoromethyl group (-CF_3 group) in the formation of different structural motifs and their influence on the crystal packing in a series of isomeric trifluoromethyl substituted benzanilides [21]. The presence of a –CF_3 group on the molecule increases the acidity of the neighboring H-atoms and thus increases the possibility of its participation in the formation of a hydrogen bond. Further, it was recently experimentally established from charge density analysis performed using high resolution X-ray data that there is an intrinsic polarization of the electron density on the fluorine atoms of the trifluoromethyl group [36]. This further increases the possibility of its participation in different intermolecular interactions like C-H···F, C-F···F-C, C-F···π in the solid state. The role of the presence of -CF_3 group in different fields of chemistry and biology are very well recognized [37-40]. The influence of the presence of -CF_3 group has also been observed in phase transitions [41] and in crystal engineering [42]. It was of interest to analyze the role and influence of CF_3 group [F-C(sp^3)] in the participation of different intermolecular interactions in the absence of any strong hydrogen bond. In the crystal structure analysis of -CF_3 substituted benzanilides, these interactions were structurally analyzed in the presence of N-H···O=C hydrogen bond. The focus is now on the removal of the H-atom connected to the N-atom, which eliminates the presence of any strong donor in the molecule, and hence eliminates the possibility of the formation of the N-H…O=C H-bond.

In this regard, a library of trifluoromethyl substituted *N*-methyl-*N*-phenylbenzamides have been synthesized (**scheme 1**) by replacing the H-atom connected to a N-atom with methyl group and their crystal structures were analyzed to investigate the nature and role of weak interactions (of the type C-H···F-C_{sp3}, C_{sp3}-F···F-C_{sp3}) in the crystal packing. Thus these compounds now eliminate the possibility of formation of any strong H-bond. The substitution of the hydrogen atom with the methyl group completely alters the molecular conformation from *trans* to *cis* geometry relative to that in benzanilides [43-45]. The change in the fluorescence and luminescence behavior with the change in its molecular conformation was very well studied by different research groups [46-48]. To get a better understanding of the nature of different intermolecular interactions, the evaluation of the stabilization energy of these interactions is of prime focus in the study. The contribution of the possible different interactions towards the crystal packing has been quantified by PIXEL [49]. The PIXEL method provides important insights towards an understanding of the crystal packing by the partitioning of the interaction energy or cohesive energy into their coulombic, polarization, dispersion and repulsion contributions. To get better insights into the different weak intermolecular interactions which are present in the crystal packing, selected molecular pairs (extracted from the crystal packing, connected with different intermolecular interactions) were analyzed. This is in contrast to the routine practice of providing details on the crystal packing related to the arrangement of molecules [50-51] on the basis of pure geometry with no inputs from energetics. On the contrary, in reality, it is the latter which contribute immensely towards crystal formation.

Experimental Section

The starting materials trifluoromethyl (-CF_3) substituted anilines and benzoyl chloride were obtained from Sigma Aldrich and were used directly from the bottle. All solvents and other reagents namely, dimethylaminopyridine (DMAP), methyl iodide (CH_3I) and sodium hydride [(NaH) 60% solution in oil] were of analytical grade. The solvents, dichloromethane (DCM) and tetrahydrofuran (THF) were dried before being used for the chemical reactions. The intermediate compounds, namely all the substituted *N*-phenylbenzamides, were synthesized in accordance with the procedure already reported in our earlier work [21].

Synthesis of substituted *N*-methyl-*N*-phenylbenzamides: In a two-neck round bottom flask, containing 1.2 equivalents of NaH, 4 ml of dry THF was added with constant stirring using the magnetic stirrer. Then 1 equiv. of the substituted *N*-phenyl benzamides was added slowly to the reaction mixture with constant stirring. Further, 3-4 ml of dry THF was added and the whole reaction mixture was refluxed for 2 hours. The reaction mixture was then allowed to come to room temperature. After this, cold methyl iodide, (excess amount, 0.6 ml added in all reactions) were added slowly to the reaction mixture with the whole flask kept over ice bath with constant stirring. After the addition, the reaction mixture was continuously stirred at room temperature for 1-2h. The progress of the reaction was monitored with thin layer chromatography (TLC). After the completion of the reaction, it was quenched with 20 ml of 5% HCl and extracted with ethyl acetate and then washed with brine solution for three times. The organic extract was further washed with saturated solution of sodium sulphite to remove the excess iodine. The organic extract was again washed with brine solution and then dried with anhydrous sodium sulphate. The crude product thus obtained was finally purified by column chromatography with ethyl acetate and hexane as eluant. The polarity of the eluant was increased slowly from 0% to 10% of ethyl acetate in hexane while performing the column. The yield was recorded after the evaporation of the solvent on completion of the column. Initially, after the column, all the compounds were obtained as thick oil (**Scheme 1**). The compounds, the compound codes being, **NM02**, **NM03**, **NM10**, **NM11**, **NM12**, **NM22**, **NM23**, **NM31** and **NM33** became solid after one day when put into the deep freeze section of the refrigerator or after recrystallization from hexane on scratching the walls of the container. The compound **NM30** was observed as a low melting solid (melting point = 39°C). The remaining synthesized compounds (five in number, **NM01**, **NM20**, **NM13**, **NM21**, **and NM32**) remained as thick oil even at -20°C.

All the synthesized compounds were characterized by FTIR [**Fig. S1(a)–(o)**, ESI], ^{1}H NMR [**Fig. S2(a)–(o)**, ESI] spectroscopy. Melting points were recorded using DSC for all the solid compounds and are given in the ESI [**Fig. S3(a)–(j)**]. Powder X-ray diffraction (PXRD) data were recorded for all the solid compounds and then compared with the simulated PXRD patterns [**Fig. S4(a)–(j)**]. The details about the product yields, melting points, spectroscopic data of all the synthesized compounds are listed in section **S1** in ESI.

The detail on all the crystallization experiments of all the solid compounds from different solvent and solvent mixtures are presented in the ESI (**Table S1**). Single crystals of all the solids except **NM30** were obtained from slow evaporation method. The compound **NM30** was observed to appear as a single crystal in the sample vial at a temperature below 25°C.

----Insert Scheme 1 here….

Scheme 1: Synthetic route for all the compounds. '**A**' and '**B**' denote the two phenyl rings from the starting material aniline and the corresponding benzoyl chloride. Compound code denoted as "**NMAB**" in this study. '**NM**' refers to *N*-methyl substitution on *N*-phenylbenzamide, **A** or **B** = 0 [no substitution on that ring] and **A** or **B** = **1**, **2**, **3** [*o*, *m*, *p* substitution of -CF_3 group on that ring respectively].

Data collection, structure solution and refinement

Single crystal X-ray diffraction data were collected on CrysAlis CCD Xcalibur, Eos (Nova), Oxford Diffraction using Mo Kα radiation (λ = 0.71073 Å) for all compounds except **NM03**, **NM22**, **NM31**. Single crystal X-ray diffraction data of **NM03**, **NM22**, **NM31** were collected on a Bruker D8 Venture diffractometer with CMOS detector using graphite monochromated Mo Kα (λ = 0.7107 Å) radiation while NM30 were collected on Bruker APEX II three circle diffractometer with CCD detector. All the data except for **NM12** were collected at 120(2)K.

All crystal structures were solved by direct methods using SIR92 [52] The non-hydrogen atoms were refined anisotropically and the hydrogen atoms bonded to C atoms were positioned geometrically and refined using a riding model with U_{iso}(H) = 1.2Ueq [C(sp^2)] and U_{iso}(H) = 1.5Ueq [C(sp^3)]. The compound NM30 was observed to be twinned at two orientations with the ratio for the BASF values being 0.59:0.41. The twin law and the corresponding HKLF5 file were generated using 'TwinRotMat' tool in WinGx [53] and refinement was performed with the HKLF5 file using SHELXL2013.

The disorder associated with the CF_3 group was modelled with PART command at two independent orientations (major component was labeled 'A') in SHELXL 2013 [54]. Molecular and packing diagrams were generated using Mercury 3.3 [55]. Geometrical calculations were done using PARST [56] and PLATON [57]. **Table 1** lists all the crystallographic and refinement data. List of selected dihedral angles were presented in **Tables 2** and **3**.

Theoretical calculations

The molecular geometry of all the compounds was optimized by DFT/B3LYP calculation with 6-31G** basis set using TURBOMOLE [58]. The experimentally obtained geometry were considered as the starting coordinates for the calculation. The molecular geometry thus obtained for the isolated molecule was compared with the experimentally observed solid state geometry (**Table 2**).

The lattice energies (**Table 4**) of all the compounds were calculated by PIXELC module in CLP computer program package (version 10.2.2012), the total energy being partitioned into their coulombic (E_{coub}), polarization (E_{pol}), dispersion (E_{disp}) and repulsion (E_{rep}) contributions. For the calculations, accurate electron densities of the molecules were obtained at MP2/6-31G** with GAUSSIAN09 [59] with H atoms at their neutron value. In case of disordered molecules, the molecular conformation with the maximum population was considered for the calculation. The interaction energy of the selected molecular pairs, extracted from the crystal packing and related by the corresponding symmetry element, was also calculated by PIXEL method (from mlc file after the calculation). The total interaction energy was partitioned into their coulombic (E_{coub}), polarization (E_{pol}), dispersion (E_{disp}) and repulsion (E_{rep}) contributions. These are listed in **Table 5** along with the selected intermolecular interactions which connect the two molecules in the molecular pair. The % dispersion energy contribution (% E_{disp}) towards the total stabilization energy was calculated as:

$\%E_{disp} = [E_{disp}/ (E_{coub} + E_{pol} + E_{disp})]*100$;

Hence, % electrostatic contribution (coulombic + polarization), $\%E_{elec} = 100 - \%E_{disp}$

These values are reported in **Table 5**.

The PIXEL interaction energy was further compared with the interaction energies obtained from theoretical calculations at DFT+Disp/B97D [60-62] level at higher aug-cc-pVTZ basis set using TURBOMOLE [63]. The hydrogen atoms were moved to neutron values (1.083 Å for C–H) before the calculations. The basis set superposition error (BSSE) for the interaction energies was corrected by using the counterpoise method [64]. The final interaction energies are listed along with the PIXEL interaction energies in **Table 5**.

Table 1: Crystallographic and refinement data

DATA	NM02	NM03	NM10	NM30	NM11
Formula	$C_{15}H_{12}NOF_3$	$C_{15}H_{12}NOF_3$	$C_{15}H_{12}NOF_3$	$C_{15}H_{12}NOF_3$	$C_{16}H_{11}NOF_6$
Formula Weight	279.26	279.26	279.26	279.26	347.26
CCDC No.	1025677	1025678	1025679	1027431	1025680
Crystal System; Space group	Monoclinic; *C*2/*c*	Monoclinic; $P2_1/c$	Orthorhombic; *Pbca*	Monoclinic; $P2_1/c$	Monoclinic; $P2_1/c$
a **(Å)**	35.8393(17)	15.1633(5)	9.6555(7)	23.731(5)	8.9803(4)
b **(Å)**	10.6270(4)	9.9603(3)	13.7420(11)	8.3394(15)	10.8526(4)
c **(Å)**	15.1660(7)	17.7768(6)	19.3339(15)	13.706(2)	14.8181(5)
α (°)/ β (°)/ γ (°)	90/ 114.399(5)/ 90	90/ 97.269(2)/ 90	90/ 90/ 90	90/ 106.707(12)/ 90	90/ 92.763(3)/ 90
Volume (Å^3) /Density (g/cm^3)	5260.3(4)/ 1.410	2663.27(15)/ 1.393	2565.3(3)/ 1.446	2597.9(8)/ 1.428	1442.49(10)/ 1.599
Z*/ *Z'	16/2	8/2	8/1	8/2	4/1
F **(000)/ *μ* (mm^{-1})**	2304/ 0.118	1152/ 0.116	1152/ 0.121	1152/ 0.119	704/0.153
θ **(min, max)**	2.34, 25.00	1.35, 27.58	2.79, 25.00	0.90, 25.01	2.75, 25.00
$h_{min,max}$, $k_{min,max}$, $l_{min,max}$	-42, 42; -12, 12; -18,18	-18, 19; -12, 11; -23, 18	-11, 11; -16, 16; -22, 22	-28, 28; -9, 9; -16, 16	-10, 10; -12, 12; -17, 17
No. of total ref./ unique ref./ obs. ref.	25157/ 4632/ 3475	22406/ 6117/ 4629	12605/ 2262/ 1743	4556/ 4556/ 3759	13687/ 2534/ 220
No. of parameters	391	395	211	364	236
R_all, R_obs	0.0635, 0.0417	0.0659, 0.0490	0.0580, 0.0398	0.0522, 0.0403	0.0434, 0.0368
wR$_2$_all, wR$_2$_obs	0.1008, 0.0888	0.1356, 0.1259	0.1028, 0.0901	0.0897, 0.0854	0.0982, 0.0933
$\Delta\rho_{min,max}$**(eÅ^{-3})**	-0.244, 0.215	-0.357, 0.381	-0.221, 0.207	-0.182, 0.223	-0.237, 0.308
G. o. F	1.050	1.061	1.055	1.063	1.043

Table 1 continued

DATA	NM12	NM22	NM23	NM31	NM33
Formula	$C_{16}H_{11}NOF_6$	$C_{16}H_{11}NOF_6$	$C_{16}H_{11}NOF_6$	$C_{16}H_{11}NOF_6$	$C_{16}H_{11}NOF_6$
Formula Weight	347.26	347.26	347.26	347.26	347.26
CCDC No.	1025681	1025682	1025683	1025684	1025685
Crystal System; Space group	Monoclinic; $P2_1/c$	Monoclinic; $P2_1/c$	Monoclinic; $P2_1/c$	Monoclinic; $P2_1/c$	Triclinic *P*-1

a **(Å)**	9.0978(7)	8.3764(5)	11.2958(5)	12.3185(10)	8.9977(4)
b **(Å)**	22.1735(15)	23.2362(17)	14.0246(4)	7.9401(5)	10.8088(5)
c **(Å)**	7.9449(5)	7.9755(6)	10.4868(3)	15.4912(12)	16.6720(9)
α (°)/ β (°)/ γ (°)	90/ 101.946(4)/ 90	90/ 103.567(2)/ 90	90/ 115.258(4)/90	90/ 90.168(4)/ 90	105.291(2)/98.901(2)/102.688(2)
Volume (Å^3) /Density (g/cm^3)	1568.02(19)/ 1.471	1509.00(18)/ 1.529	1502.48(9)/ 1.535	1515.19(19)/ 1.522	1486.36(12)/ 1.552
Z/ Z′	4/1	4/1	4/1	4/1	4/2
F **(000)/ *μ* (mm^{-1})**	704/ 0.141	704/ 0.146	704/ 0.147	704/ 0.146	704/ 0.149
θ **(min, max)**	1.84, 25.00	2.65/ 25.00	2.47/ 25.00	2.63/ 25.00	1.30/ 30.67
$h_{min,max}$, $k_{min,max}$, $l_{min,max}$	-10, 9; -22, 26; -9, 9	-9, 8; -27, 27; -9, 9	-13, 13; -16, 16; -12, 12	-14, 13; -9, 9; -18, 18	-11, 12; -15, 15; -23, 14
No. of total ref./ unique ref./ obs. ref.	13654/ 2767/ 2117	21987/ 2652/ 2199	14260/ 2649/ 2238	11173/ 2683/ 2044	30219/ 9103/ 7006
No. of parameters	247	246	250	246	491
R_all, R_obs	0.0637, 0.0482	0.0534, 0.0410	0.0499, 0.0411	0.0590, 0.0384	0.0602/ 0.0430
wR_2_all, wR_2_obs	0.1388, 0.1285	0.1059, 0.0993	0.1065, 0.0993	0.0930, 0.0865	0.1143/ 0.1040
$\Delta\rho_{min,max}$(eÅ^{-3})	-0.222, 0.363	-0.343, 0.497	-0.339, 0.398	-0.239, 0.215	-0.380, 0.446
G. o. F	1.066	1.033	1.066	1.034	1.039

Table 2: List of selected dihedral angles (°) and geometry of intramolecular weak C(sp^3)-H···O=C hydrogen bond and their comparison with the values obtained at DFT/B3LYP calculation (in *italic*).

	Angle 1(°) Plane1/2	**Angle 2(°) Plane1/3**	**Angle 3(°) Plane2/3**	**Geometry of C(sp^3)-H···O (Å, °)**
NM00	67.4(1) *67.3*	47.1(1) *32.9*	62.5(1) *60.1*	2.47, 93 *2.42, 90*
NM02	66.9(1)/ 64.9(1)′ *70.3/ 69.9′*	46.0(1)/ 53.5(1)′ *34.3/ 36.6′*	65.4(1)/ 62.6(1)′ *70.9/ 62.1′*	2.32, 102/ 2.39, 97′ *2.50, 87; 2.42, 91′*
NM03	58.6(1)/ 71.9(1)′ *65.5/ 67.0*	44.0(1)/ 43.5(1)′ *39.2/ 38.8*	59.8(1)/ 70.2(1)′ *57.1/ 61.0*	2.31, 100/ 2.27, 104′ *2.23, 106/ 2.51, 86′*
NM10	69.8(1) *76.3*	39.2(1) *38.9*	67.9(1) *77.1*	2.28, 102 *2.33, 97*
NM30	57.4(1)/ 55.5(1)′ *68.0/ 65.5*	43.7(1)/ 43.4(1)′ *36.4/ 32.7*	48.8(1)/ 53.6(1)′ *58.4/ 54.8*	2.37, 94/ 2.65, 80′ *2.37, 96/ 2.46, 87*
NM11	1.7(1) *4.6*	84.9(1) *84.4*	85.6(1) *85.5*	-----
NM12	73.7(1) *76.1*	58.9(1) *39.4*	84.4(1) *77.5*	2.56, 87 *2.32, 98*
NM22	62.3(1) *67.7*	65.4(1) *33.9*	64.8(1) *59.1*	2.41, 97 *2.42, 91*
NM23	69.1(1) *66.3*	50.5(1) *34.6*	66.3(1) *58.5*	2.34, 102 *2.43, 90*
NM31	61.4(1) *67.9*	61.2(1) *59.8*	61.5(1) *57.8*	2.43, 92 *2.24, 106*

NM33	69.5(1)/ 72.9(1)' *65.9/ 68.6*	34.1(1)/ 62.4(1)' *38.3/ 46.5*	56.7(1)/ 65.5(1)' *57.6/ 62.3*	2.38, 94/ 2.40, 98' *2.37, 97/ 2.42, 98'*

(') denotes the second molecule in the asymmetric unit.

Table 3: List of related structures, reported in CSD along with their space group, cell parameters and dihedral angles (as reported in **Table 2).**

Ref Code	**Space group, *Z***	**Cell Parameters, a, b, c (Å) / α, β, γ (°)**	**Angle 1(°)**	**Angle 2(°)**	**Angle 3(°)**
JAZJOJ10[43] **(NM00)**	*Pbca*, *Z*=8	12.5881, 12.3092, 14.6542/ 90, 90, 90	----	----	----
YEGKIE[43]	$P2_1nb$, Z =4	11.308(1), 15.878(2), 6.876(5)/ 90, 90, 90	70.8	36.7	65.0
YEGLAX[43]	*P*-1, Z = 2	11.602, 12.766(4), 7.372(1)/ 92.19(3), 104.93(2), 137.31(1)	72.6	62.1	83.3
YEGKEA[43]	$P2_1/a$, Z = 4	13.257(7), 13.234(11), 8.005(1)/ 90, 98.01(1), 90	65.9	76.6	62.8
YEGKOK[43]	$P2_1/n$, Z = 4	14.909(1), 6.795(2), 13.358(1), 90, 98.46(1), 90	67.5	43.7	75.2
YEGJEY[43]	*Cc*, *Z* = 4	15.250(3), 7.502(1), 13.733(3), 90, 106.77(2), 90	1.06	85.5	85.1
DIBGIF[65]	$P2_1/n$, *Z* = 4	7.123(3), 16.792(8), 13.785(7), 90, 102.881, 90	16.5	85.3	84.3
DIBGAX[65]	*Pc*, *Z* = 8, *Z'* = 4	11.1542(10), 8.4970(7), 31.528(3), 90, 95.122(2), 90	11.0	87.7	76.9

[43]Azumaya *et al*., 1994; [65]Cockroft *et al*., 2007

Table 4: Lattice energy (kJ/mol) partitioned into Coulombic, polarization, dispersion and repulsion contributions by PIXEL method.

	E_{Coul}	E_{Pol}	E_{Disp}	E_{Rep}	E_{Tot}
NM00	-30.3	-15.5	-123.0	65.5	-103.3
NM02	-38.0	-14.8	-120.7	66.3	-107.2
NM03	-42.3	-16.0	-119.6	75.1	-102.8
NM10	-45.5	-16.4	-122.4	69.4	-114.9
NM30	-35.5	-13.4	-122.9	66.4	-105.5
NM11[a]	-34.6	-13.9	-122.9	64.3	-107.1
NM12	-36.4	-13.5	-97.9	46.0	-101.9
NM22	-46.7	-19.7	-119.6	77.2	-108.7
NM23	-40.8	-15.9	-122.7	70.9	-108.5
NM31	-38.6	-12.8	-111.2	57.2	-105.4
NM33	-45.7	-16.8	-125.7	78.8	-109.3
YEGLAX	-35.2	-13.5	-129.2	67.0	-117.8
YEGKEA	-30.3	-15.6	-116.4	61.8	-100.4
YEGKOK	-35.9	-14.8	-127.4	71.9	-106.2

YEGJEY[a]	-32.8	-13.6	-142.6	78.5	-110.5

[a] Molecules exist in *trans* conformation

Table 5: List of Interaction energies (kJ/mol) of molecular pairs related by symmetry operation along with possible involved intermolecular interactions.

[a] Pair/ Motif	Symmetry code	Centroid-Centroid Distance (Å)	E_{Coul}	E_{Pol}	E_{Disp} [b]	E_{Rep}	E_{Tot}	DFT-D2/ B97-D (BSSE corrected)	Possible Involved Interactions [c]	Geometry (Å/ °) D(D…A), d(H…A), ∠ D-H…A
NM00 (*Pbca*, Z′ = 1; Ref code: JAZJOJ10)										
I	-x+3/2, y+1/2, z	6.320	-9.1	-7.7	-33.1 (66)	25.4	-24.5	-28.4	C6-H6⋯O1 C14-H14C⋯C5 (π)	3.271(1)/ 2.41/ 136 3.757(1)/ 2.98/ 129
II	x-+1/2, -y+1/2, -z+1	6.877	-5.3	-2.1	-25.7 (78)	13.6	-19.6	-24.3	C3-H3⋯C9 (π) C2-H2⋯C11 (π) H14A⋯H9	3.911(1)/ 2.96/ 147 3.664(1)/ 2.99/121 2.38
III	x-1/2, y, -z+3/2	7.885	-5.0	-2.5	-19.6 (72)	9.8	-17.2	-19.7	C12-H12⋯C4 (π) C14-H14A⋯C3 (π)	3.880(1)/ 2.98/ 140 3.787(1)/ 2.97/ 133
IV	x, -y+1/2, z-1/2	7.397	-4.5	-2.5	-11.5 (62)	4.7	-13.9	-15.8	C9-H9⋯C2 (π) C9-H9⋯O1	4.082(1)/ 3.14/ 147 3.361(1) 2.89/ 106
V	-x+2, y+1/2, -z+3/2	9.167	-3.7	-1.8	-8.8 (62)	4.2	-10.1	-11.3	C4-H4⋯O1	3.907(1)/ 2.86/ 163
VI	-x+2, -y+1, -z+1	7.527	0.6	-1.1	-15.4 (97)	5.8	-10.1	-11.2	C10-H10⋯C4 (π)	3.936(1)/ 3.18/ 128
VII	-x+3/2, -y+1, z-1/2	9.065	-1.8	-0.6	-7.9 (77)	2.9	-7.3	-8.4	C10-H10⋯C6 (π) C10-H10⋯C5 (π)	4.037(1)/ 3.11/ 144 3.836(1)/ 3.18/ 120
NM02 (*C*2/*c*, Z′ = 2)										
I 1⋯1	-x+1/2, -y+1/2, -z	7.800	-17.8	-5.4	-30.5 (57)	18.6	-35.1	-43.2	C12-H12⋯O1 C14-H14B⋯O1	3.790(3)/ 2.77/ 158 3.610(3)/ 2.83/129
II 2⋯2	-x+1, y, -z+1/2	5.505	-8.8	-4.6	-44.2 (77)	26.1	-31.5	-31.0	C4′⋯C4′ (π⋯π) C5′⋯C5′ (π⋯π) C5′-H5′⋯C11′ (π)	3.431(2) 3.393(2) 3.772(2)/ 2.78/ 153
III 1⋯2	x, -y, z+1/2	6.175	-14.5	-6.0	-30.1 (59)	19.5	-31.1	-35.4	C8-H8⋯O1′ C6′-H6′⋯F1 C8′-H8′⋯F1	3.393(2)/ 2.46/ 144 3.313(2)/ 2.43/ 138 3.400(3)/ 2.65/ 126
IV 1⋯1	-x+1/2, y+1/2, -z+1/2	7.260	-11.4	-4.6	-36.2 (69)	22.2	-30.0	-35.3	C10-H10⋯O1 C5-H5⋯Cg2 (π)	3.429(3)/ 2.67/ 127 3.670(2)/ 2.65/ 157
V 1⋯2	x, y, z	5.450	-6.3	-4.8	-23.7 (68)	12.4	-22.4	-27.9	C2′-H2′⋯O1 C15-F1⋯F1A′-C15′	3.356(3)/ 2.45/ 141 2.823(2)/ 98(1)/ 158(1)
VI 1⋯2	-x+1/2, -y+1/2, -z	8.499	-8.3	-4.0	-14.9 (55)	9.5	-17.6	-18.2	C11-H11⋯O1′ C12-H12⋯O1′ C14-H14B⋯F1A′	3.312(3)/ 2.58/ 125 3.428(2)/ 2.84/ 115 3.623(7)/ 2.68/ 146
VII 1⋯2	x, y-1, z	8.941	-4.6	-1.1	-14.4 (72)	5.4	-14.7	-18.4	C9′-H9′⋯F2 C4⋯C9′ (π⋯π)	3.300(3)/ 2.71/ 114 3.802(2)
VIII 2⋯2	x, -y, z+1/2	7.593	-5.6	-2.2	-17.7 (69)	11.0	-14.5	-18.5	C10′-H10′⋯C4′ (π) C11′-H11′⋯C1′ (π)	3.609(2)/ 2.78/ 133 4.008(2)/ 2.99/ 157
IX 2⋯2	x, y-1, z	10.627	-5.4	-1.7	-10.2 (59)	7.3	-10.1	-10.7	C14′-H14E⋯F1A′ C8′-H8′⋯F2A′ C8′-H8′⋯F3A′	3.541(8)/ 2.51/ 160 3.253(11)/ 2.58/ 120 3.797(9)/ 2.74/ 166
X 1⋯2	-x+1, -y, -z+1	10.441	-2.3	-0.6	-6.2 (68)	2.0	-7.1	-8.3	C10′-H10′⋯F3 C10′-H10′⋯F2	3.829(2)/ 2.86/ 149 3.800(2)/ 2.89/ 142
XI 1⋯2	-x+1, y, -z+1/2	9.365	-2.6	-1.0	-7.6 (68)	4.3	-7.0	-8.1	C4′-H4′⋯F2 C4′-H4′⋯F3	3.619(3)/ 2.66/ 147 3.306(3)/ 2.68/ 117
NM03 ($P2_1/c$, Z′ = 2)										

I 1⋯2	**x, y, z**	**5.173**	**-23.0**	**-8.0**	**-41.3 (57)**	**33.0**	**-39.3**	**-52.0**	**C12-H12⋯O1′ C14-H14B⋯O1′ C6⋯C5′ (π⋯π) C6⋯C6′ (π⋯π)**	**3.297(2)/ 2.26/ 161 3.448(2)/ 2.66/ 129 3.387(1) 3.481(1)**
II 2⋯2	**-x, y-1/2, -z+1/2**	**6.506**	**-17.2**	**-7.3**	**-46.7 (65)**	**36.1**	**-35.1**	**-42.1**	**C10′-H10′⋯O1′ C5′-H5′⋯Cg2′ (π) C8′-H8′⋯C11′ (π)**	**3.340(2)/ 2.45/ 139 3.523(2)/ 2.49/ 159 3.799(2)/ 2.80/ 154**
III 1⋯1	**-x+1, -y, -z**	**6.565**	**-9.7**	**-4.4**	**-41.5 (75)**	**27.9**	**-27.6**	**-33.4**	**C10-H10⋯Cg1(π) C9⋯C9 (π⋯π) C9⋯C10 (π⋯π)**	**3.834(1)/ 2.89/ 146 3.245 3.430**
IV 1⋯2	**x, -y+1/2, z+1/2**	**7.758**	**-8.3**	**-3.7**	**-28.6 (70)**	**17.0**	**-23.6**	**-28.6**	**C3′-H3′⋯C10 (π)**	**3.860(1)/ 2.79/ 170**
V 1⋯2	**-x, -y, -z**	**8.970**	**-9.9**	**-4.7**	**-20.4 (58)**	**14.7**	**-20.3**	**-21.8**	**C12′-H12′⋯O1**	**3.404(2)/ 2.33/ 173**
VI 1⋯2	**-x, y+1/2, -z+1/2**	**8.380**	**-7.8**	**-2.9**	**-16.1 (60)**	**10.9**	**-15.9**	**-18.6**	**C9′-H9′⋯O1 C10′-H10′⋯C3(π)**	**3.614(2)/ 2.69/ 143 3.605(1)/ 2.71/ 139**
VII 1⋯2	**x, y-1, z**	**8.775**	**-8.0**	**-2.3**	**-8.8 (46)**	**4.6**	**-14.5**	**-16.7**	**C3-H3⋯O1′ C2′-H2′⋯F2A**	**3.393(2)/ 2.57/ 132 3.721(3)/ 2.69/ 160**
VIII 1⋯2	**x, -y-1/2, z-1/2**	**8.192**	**-4.5**	**-1.4**	**-9.3 (61)**	**6.0**	**-9.2**	**-10.7**	**C2-H2⋯F1A′ C3-H3⋯F1A′**	**3.111(3)/ 2.54/ 112 3.241(2)/ 2.81/ 104**
IX 1⋯1	**-x+1, y+1/2, -z+1/2**	**8.594**	**-2.2**	**-0.9**	**-8.2 (73)**	**3.7**	**-7.6**	**-10.7**	**C5-H5⋯F3A**	**3.527(4)/ 2.46/ 172**
X 1⋯1	**-x, -y, -z**	**10.564**	**-2.6**	**-1.6**	**-4.1 (49)**	**1.0**	**-7.3**	**-8.8**	**C14-H14C⋯O1**	**3.987(2)/ 2.96/ 159**
XI 1⋯1	**x, -y-1/2, z-1/2**	**9.340**	**-2.8**	**-0.7**	**-5.7 (62)**	**3.2**	**-6.0**	**-7.2**	**C9-H9⋯F2A C8-H8⋯F2A**	**3.259(3)/ 2.60/ 118 3.386(3)/ 2.89/ 109**
XII 1⋯2	**-x+1, y+1/2, -z+1/2**	**10.943**	**-2.8**	**-0.4**	**-3.8 (54)**	**1.4**	**-5.6**	**-6.8**	**C11-H11⋯F2A′**	**3.555(3)/ 2.64/ 142**
NM10 (*Pbca*, Z′ = 1)										
I	**-x+1, -y, -z+1**	**5.968**	**-16.2**	**-6.2**	**-34.2 (60)**	**20.2**	**-36.2**	**-41.3**	**C11-H11⋯C5 (π)**	**3.775(1)/ 2.74/ 161**
II	**x-1/2, y, -z+3/2**	**7.490**	**-11.3**	**-5.8**	**-31.4 (65)**	**20.5**	**-28.1**	**-33.4**	**C14-H14B⋯O1 C8-H8⋯C6 (π)**	**3.382(2)/ 2.59/ 130 3.951(1)/ 2.90/ 164**
III	**-x+1/2, y-1/2, z**	**7.881**	**-9.1**	**-2.6**	**-18.7 (62)**	**9.9**	**-20.6**	**-22.9**	**C9-H9⋯F3A C10-H10⋯F3A C14-H14C⋯C10 (π)**	**3.378(15)/ 2.69/ 121 3.409(15)/ 2.76/ 119 3.974(2)/ 3.05/ 144**
IV	**x-1/2, -y+1/2, -z+1**	**6.713**	**-4.8**	**-1.5**	**-16.5 (72)**	**5.4**	**-17.4**	**23.0**	**C14-H14C⋯F2A C2-H2⋯F1A C3-H3⋯F1A**	**3.670(10)/ 2.72/ 146 3.335(11)/ 2.79/ 111 3.338(12)/ 2.79/ 112**
V	**-x+1, y-1/2, -z+3/2**	**8.997**	**-7.2**	**-3.7**	**-10.8 (50)**	**10.1**	**-11.7**	**-11.4**	**C5-H5⋯O1**	**3.310(2)/ 2.42/ 139**
VI	**-x+3/2, y-1/2, z**	**8.989**	**-4.4**	**-2.1**	**-8.0 (55)**	**4.9**	**-9.6**	**-11.2**	**C4-H4⋯O1**	**3.567(2)/ 2.50/ 169**
VII	**x+1, y, z**	**9.655**	**-0.5**	**-1.7**	**-11.8 (84)**	**7.1**	**-6.9**	**-10.8**	**C3-H3⋯C8 (π)**	**3.839(2)/ 2.83/ 155**
NM30 (*P*2$_1$/*c*, Z′ = 2)										
I 1⋯2	**x, y, z**	**7.321**	**-11.4**	**-5.4**	**-31.2 (65)**	**22.4**	**-25.6**	**-32.3**	**C3'-H3'⋯O1 C2'-H2'⋯C1 C13⋯C3 (π⋯π)**	**3.403(4)/ 2.65/ 127 3.727(3)/ 2.97/ 127 3.575(3)**
II 2⋯2	**x, -y+1/2, z+1/2**	**8.623**	**-8.0**	**-4.1**	**-17.7 (59)**	**11.0**	**-18.8**	**-19.6**	**C8'-H8'⋯O1'**	**3.359(3)/ 2.53/ 133**
III 1⋯1	**x, -y+3/2, z+1/2**	**8.686**	**-8.4**	**-3.9**	**-17.0 (58)**	**11.0**	**-18.3**	**-19.6**	**C12-H12⋯O1**	**3.352(4)/ 2.49/ 136**
IV	**x, -y+3/2, z-1/2**	**7.524**	**-5.2**	**-2.0**	**-23.9**	**12.8**	**-18.3**	**-21.8**	**C12'-H12'⋯F1'**	**3.385(3)/ 2.63/ 126**

2···2					(77)				C4'···C9' (π···π) C5'···C9' (π···π)	3.547(3) 3.408(3)
V 1···1	x, -y+1/2, z-1/2	7.482	-5.8	-2.3	-25.0 (76)	14.9	-18.2	-17.2	C8-H8···F2 C3···C11 (π···π) C4···C11 (π···π)	3.379(4)/ 2.62/ 127 3.346(3) 3.528(3)
VI 1···2	x, -y+3/2, z+1/2	8.400	-4.6	-3.4	-22.2 (74)	13.2	-17.0	-21.1	C4'-H4'···C6 (π) C4'···C13	3.758(3)/ 2.83/ 144 3.685(3)
VII 2···2	-x, -y+1, -z+1	7.998	-6.1	-1.6	-18.3 (70)	8.9	-17.0	-22.1	C15'-F2'···C9' (π)	3.713(3)/ 3.155(2)/ 104(1)
VIII 1···1	-x+1, -y+1, -z+2	8.078	-5.9	-1.4	-18.2 (71)	9.2	-16.4	-21.3	C15-F3···C11 (π)	3.693(3)/ 3.161(2)/ 102
IX 2···2	-x, y-+1/2, -z+1/2	6.529	-3.6	-1.8	-19.0 (78)	8.4	-16.0	-19.8	C12'-H12'···F2' C15'-F2'···C13'=O1'	3.338(3)/ 2.52/ 132 4.517(3)/3.203(2)/166(1)
X 1···1	-x+1, y-+1/2, -z+3/2	6.520	-3.4	-1.8	-18.1 (78)	7.8	-15.5	-19.3	C8-H8···F3 C15-F3···C13=O1	3.330(3)/ 2.54/ 129 4.473(3)/3.154(2)/166(1)
XI 1···1	x, y+1, z	8.339	-6.0	-2.1	-11.7 (59)	4.9	-14.9	-17.3	C4-H4···O1 C14-H14B···F1	3.547(4)/ 2.73/ 132 3.637(3)/ 2.68/ 147
XII 2···2	x, y-1, z	8.339	-6.2	-2.5	-12.3 (59)	6.4	-14.6	-17.2	C4'-H4'···O1' C14'-H14E'···F3'	3.515(4)/ 2.66/ 135 3.495(4)/ 2.59/ 141
XIII 1···2	x, -y+1/2, z+1/2	8.349	-4.4	-3.1	-13.0 (63)	7.9	-12.6	-13.8	C5-H5···C6' (π) C5'-H5'···O1'	3.722(3)/ 2.73/ 152 3.499(5)/ 2.91/ 114
XIV 2···2	-x, -y+2, -z+1	10.740	1.6	-0.3	-5.2 (95)	2.1	-1.8	-2.5	C15'-F2'···F3'-C15' C15'-F3'···F3'-C15'	3.104(2)/ 90(1)/ 128(1) 3.002(2)/ 94(1)/ 94(1)
XV 1···1	-x+1, -y, -z+2	10.759	1.6	-0.3	-5.1 (94)	1.9	-1.8	-2.6	C15-F1···F1-C15	2.966(2)/ 94(1)/ 94(1)
NM11 (*P*2$_1$/*c*, Z′ = 1)										
I	-x+1, -y, -z+2	7.697	-27.0	-7.9	-29.4 (46)	23.4	-40.8	-43.4	C9-H9···O1 C10-H10···F6	3.498(2)/ 2.46/ 160 3.296(2)/ 2.49/ 144
II	x-1, y, z	8.980	-7.7	-2.6	-29.4 (74)	17.6	-22.0	-31.3	C10···C3 (π···π) C11···C4 (π···π)	3.560(2) 3.579(2)
III	-x+2, -y+1, -z+2	8.424	0.1	-1.6	-24.9 (94)	8.6	-17.8	-23.3	C2···C3 (π···π) C16···C4 (π···π)	3.960(2) 3.955(2)
IV	x, -y+1/2, z-1/2	7.409	-4.6	-1.5	-17.4 (74)	6.7	-16.7	-21.0	C5-H5···F6 C6-H6···F4	3.543(2)/ 2.79/ 127 3.773(2)/ 2.82/ 148
V	-x+2, y+1/2, -z+3/2	8.484	-11.8	-3.9	-10.7 (41)	9.9	-16.6	-18.2	C5-H5···O1 C4-H4···F3	3.287(2)/ 2.35/ 144 3.645(2)/ 2.65/ 154
VI	-x+1, y+1/2, -z+3/2	7.347	0.6	-2.5	-23.7 (93)	9.8	-15.8	-21.0	C14-H14A···F1 C14-H14A···F3 C10-H10···C5 (π)	3.305(2)/ 2.84/ 106 3.731(2)/ 2.87/ 137 3.871(2)/ 3.11/ 128
VII	x-1, -y+1/2, z-1/2	11.364	-2.3	-0.5	-6.3 (69)	3.8	-5.3	-7.5	C11-H11···F5 C3-H3···F1	3.600(2)/ 2.58/ 156 3.727(2)/ 2.78/ 147
NM12 (*P*2$_1$/*c*, Z′ = 1)										
I	-x+2, -y+2, -z	5.674	-6.7	-3.9	-41.4 (80)	15.7	-36.2	-45.0	C10-H10···C3 (π) C9-H9···C5 (π) C9 ···C9 (π···π) C15-F1···F4A-C16	3.821(2)/ 3.02/ 131 4.077(1)/ 3.04/ 160 3.624(2) 3.074(3)/ 140(1)/ 112(1)
II	x, -y+3/2, z-1/2	7.061	-12.9	-7.1	-21.8 (52)	16.2	-25.6	-31.2	C12-H12···O1 C6-H6···O1	3.356(3)/ 2.32/ 160 3.562(3)/ 2.57/ 153
III	x, y, z-1	7.945	-8.9	-2.5	-16.5 (59)	5.7	-22.3	-25.9	C11-H11···O1 C10-H10···F2	3.646(3)/ 2.66/ 152 3.446(3)/ 2.69/ 127
IV	x-1, y, z	9.098	-4.0	-1.6	-17.5 (76)	7.3	-15.8	-20.7	C14-H14B···C3 (π) C3-H3···F1	4.000(2)/ 2.96/ 162 3.751(3)/ 2.78/ 149
V	-x+2, -y+2, -z+1	7.883	-3.1	-0.9	-12.1 (75)	4.1	-12.1	-16.0	C2-H2···F1	3.427(3)/ 2.63/ 130

VI	x-1, y, z-1	10.768	0.2	-0.4	-4.9 (96)	1.3	-3.8	-6.1	C14-H14A···F5A C15-F3···F4A-C16	3.814(9)/ 2.85/ 149 3.061(8)/ 166(2)/ 156(2)
NM22 ($P2_1/c$, Z′ = 1)										
I	x, -y+1/2, z+1/2	7.291	-24.7	-10.9	-32.9 (48)	31.5	-37.0	-40.5	C2-H2···O1 C8-H8···O1 C6-H6···O1	3.500(2)/ 2.43/ 173 3.118(2)/ 2.21/ 140 3.679(3)/ 2.69/ 152
II	-x+1, -y+1, -z	5.937	-2.9	-4.7	-42.8 (85)	24.3	-26.0	-33.4	C10-H10···C5 (π) C10···C10 (π···π)	3.837(2)/ 2.79/ 163 3.500(1)
III	x-1, y, z	8.376	-10.2	-4.6	-30.0 (67)	20.6	-24.2	-30.3	C4-H4···Cg2 (π) C5-H5···F2A	3.475(1)/ 2.51/ 148 3.583(14)/ 2.67/ 142
IV	x, y, z+1	7.976	-6.2	-2.6	-17.9 (67)	11.2	-15.6	-18.1	C12-H12···F1A C6-H6···F6	3.145(15)/ 2.25/ 139 3.352(2)/ 2.58/ 128
V	-x+1, -y+1, -z+1	8.023	-3.1	-0.8	-7.7 (66)	1.4	-10.2	-14.6	C11-H11···F5 C11-H11···F6	3.815(2)/ 2.91/ 142 3.882(2)/ 2.99/ 140
NM23 ($P2_1/c$, Z′ = 1)										
I	-x+1, -y+1, -z	5.065	-15.0	-9.3	-58.3 (71)	43.4	-39.1	-50.8	C10-H10···Cg1 (π) C10···C11 (π···π)	3.652(2)/ 2.61/ 161 3.331(2)
II	-x+1, -y+1, -z+1	7.982	-18.4	-8.1	-37.1 (58)	25.0	-38.7	-42.4	C12-H12···O1 C2-H2···O1	3.652(2)/ 2.58/ 172 3.552(2)/ 2.80/ 126
III	x, -y+1/2, z-1/2	6.205	-14.6	-5.6	-27.6 (58)	16.3	-31.4	-38.7	C5-H5···O1 C2-H6···O1	3.314(2)/ 2.62/ 121 3.302(2)/ 2.60/ 122
IV	-x+1, y+1/2, -z+1/2	7.260	-4.6	-2.3	-18.6 (73)	11.3	-14.2	-19.0	C14-C14C···F5A C5···C12 (π···π)	3.636(2)/ 2.62/ 157 3.457(2)
V	x-1, -y+1/2, z-1/2	10.749	-2.0	-0.7	-8.4 (76)	3.1	-8.0	-10.6	C8-C8···F4A C15-F3A···F6A-C16	3.700(3)/ 2.64/ 166 2.948(2)/148(1)/96(1)
VI	x+1, y, z+1	11.682	-2.1	-0.6	-6.7 (71)	3.9	-5.5	-6.6	C3-H3···F1A C15-F3A···F4A-C16	3.550(2)/ 2.48/ 173 3.004(2)/96(1)/145(1)
NM31 ($P2_1/c$, Z′ = 1)										
I	-x+1, y-1/2, -z+1/2	7.187	-11.9	-4.9	-32.8 (66)	19.5	-30.1	-36.8	C4-H4···O1 C4···C1 (π···π) C3···C6 (π···π)	3.410(2)/ 2.42/ 151 3.665(2) 3.656(2)
II	x, y-1, z	7.940	-12.5	-3.6	-17.2 (52)	11.3	-22.1	-26.0	C9-H9···O1 C6-H6···F3A C12-H12···F1A C14-H14A···F1A	3.508(2)/ 2.54/ 149 3.229(7)/ 2.38/ 135 3.699(6)/ 2.72/ 150 3.656(7)/ 2.74/ 143
III	-x, -y, -z+1	9.001	-5.5	-1.5	-18.7 (73)	6.2	-19.6	-24.9	C11···C11 (π···π) C14-H14B···F2A	3.595(2) 3.600(6)/ 2.90/ 123
IV	x, -y+1/2, z+-1/2	8.143	-5.5	-3.3	-20.1 (70)	10.8	-18.2	-19.5	C11-H11···O1 C5-H5···F6 C6-H6···F6	3.692(2)/ 2.76/ 145 3.244(2)/ 2.52/ 123 3.280(2)/ 2.61/ 120
V	-x, y+1/2, -z+1/2	7.937	-6.5	-2.1	-15.2 (64)	9.6	-14.2	-19.4	C14-H14C···Cg2 (π)	3.939(2)/ 3.05/ 139
VI	-x+1, -y, -z+1	8.313	-0.7	-0.8	-9.6 (86)	1.9	-9.2	-13.8	C4-H4···F2A	3.614(5)/ 2.80/ 133
VII	x, -y-1/2, z-+1/2	9.458	-0.0	-0.3	-6.3 (95)	1.7	-4.9	-7.6	C15-F3A···F6-C16	2.918(2)/134(1)/111(1)
NM33 (P-1, Z′ = 2)										
I 1···1	-x+1, -y+1, -z	7.358	-17.3	-8.1	-38.8 (60)	26.4	-37.8	-40.8	C8-H8···O1	3.562(1)/ 2.49/ 173
II 1···2	-x+1, -y+1, -z	4.361	-10.6	-8.0	-57.2 (75)	40.6	-35.3	-49.8	C3′-H3′···Cg1 (π) C9-H9···C8′ (π) C8···C3′ (π···π) C9···C3′ (π···π)	3.664(2) /2.63/ 159 3.648(1)/ 2.95/ 122 3.486(2) 3.311(2)

III 2···2	-x+1, -y+1, -z+1	6.426	-12.7	-3.8	-32.5 (66)	16.0	-33.0	-37.1	C6′-H6′···F2A′ C6′-H6′···F1A′ C5′-H5′···F1A′ C11′···C11′ (π···π)	3.772(10)/ 2.72/ 166 3.475(7)/ 2.72/ 127 3.544(8)/ 2.88/ 120 3.547(2)
IV 1···2	x, y, z	8.192	-21.1	-6.9	-19.4 (41)	19.2	-28.2	-29.3	C8′-H8′···O1 C2′-H2′···O1	3.370(2)/ 2.30/ 169 3.285(2)/ 2.42/ 136
V 1···2	-x, -y+1, -z	8.726	-8.3	-4.7	-26.4 (67)	17.6	-21.9	-28.2	C14-H14C···O1′ C14-H14B···C2′ (π) C11···C5′ (π···π)	3.636(2)/ 2.80/ 134 3.502(2)/ 2.63/ 138 3.674(2)
VI 1···1	-x+1, -y, -z	7.963	-5.6	-2.4	-28.8 (78)	17.4	-19.4	-29.7	C4···C5 (π···π) C16···C6 (π···π)	3.541(1) 3.615(1)
VII 1···2	x+1, y, z	10.529	-14.9	-5.0	-10.5 (35)	15.5	-15.0	-14.6	C3-H3···O1′ C14′-H14F···F5	3.167(1)/ 2.20/ 148 3.542(2)/ 2.81/ 125
VIII 2···2	x-1, y, z	8.998	-6.3	-1.1	-10.3 (58)	3.8	-14.0	-17.7	C14′-H14D···F3A′ C15′-F3A′···C13′=O1′	3.275(11)/ 2.75/ 110 3.179(10)/ 177
IX 1···1	x-1, y, z	8.998	-3.1	-1.5	-11.6 (72)	6.1	-10.0	-13.1	C12-H12···F6 C14-H14B···F6	3.397(2)/ 2.43/ 148 3.311(2)/ 2.77/ 111
X 1···1	-x, -y, -z-1	11.332	-4.0	-0.7	-8.4 (64)	3.2	-10.0	-11.5	C11-H11···F6 C15-F2···F3-C15	3.762(1)/ 2.78/ 151 3.009(1)/130(1)/99(1)
XI 1···2	-x+1, -y, -z	8.377	-4.4	-1.5	-11.9 (67)	7.9	-10.0	-13.8	C14′-H14F···F6 C14′-H14F···F4	3.509(2)/ 2.48/ 160 3.654(2)/ 2.76/ 140
XII 1···2	x, y, z-1	10.301	-3.8	-1.1	-7.9 (62)	4.9	-8.0	-9.5	C11′-H11′···F1 C12′-H12′···F1 C12′-H12′···F2	3.210(2)/ 2.54/ 119 3.262(2)/ 2.66/ 115 3.899(1)/ 2.90/ 153
XIII 2···2	-x+1, -y+2, -z+1	9.320	-2.9	-0.4	-5.6 (63)	1.8	-7.2	-10.7	C5′-H5′···F5A′	3.682(7)/ 2.78/ 141
XIV 1···1	-x+2, -y, -z	13.180	1.1	-0.2	-4.7 (96)	2.7	-1.2	-1.5	C16-F5···F6-C16 C16-F5···F5-C16	3.012(1)/ 139(1)/95(1) 2.889(1)/101(1)/101(1)

[a]Arranged in descending order of energy; [b] Values in parenthesis represent % dispersion energy contribution (% E_{disp}) towards the total stabilization, % electrostatic contribution (% E_{elec}) = 100 – % E_{disp}; [c]Cg1 and Cg2 refer to the centre of gravity for phenyl rings C1-C6 and C7-C12 respectively.

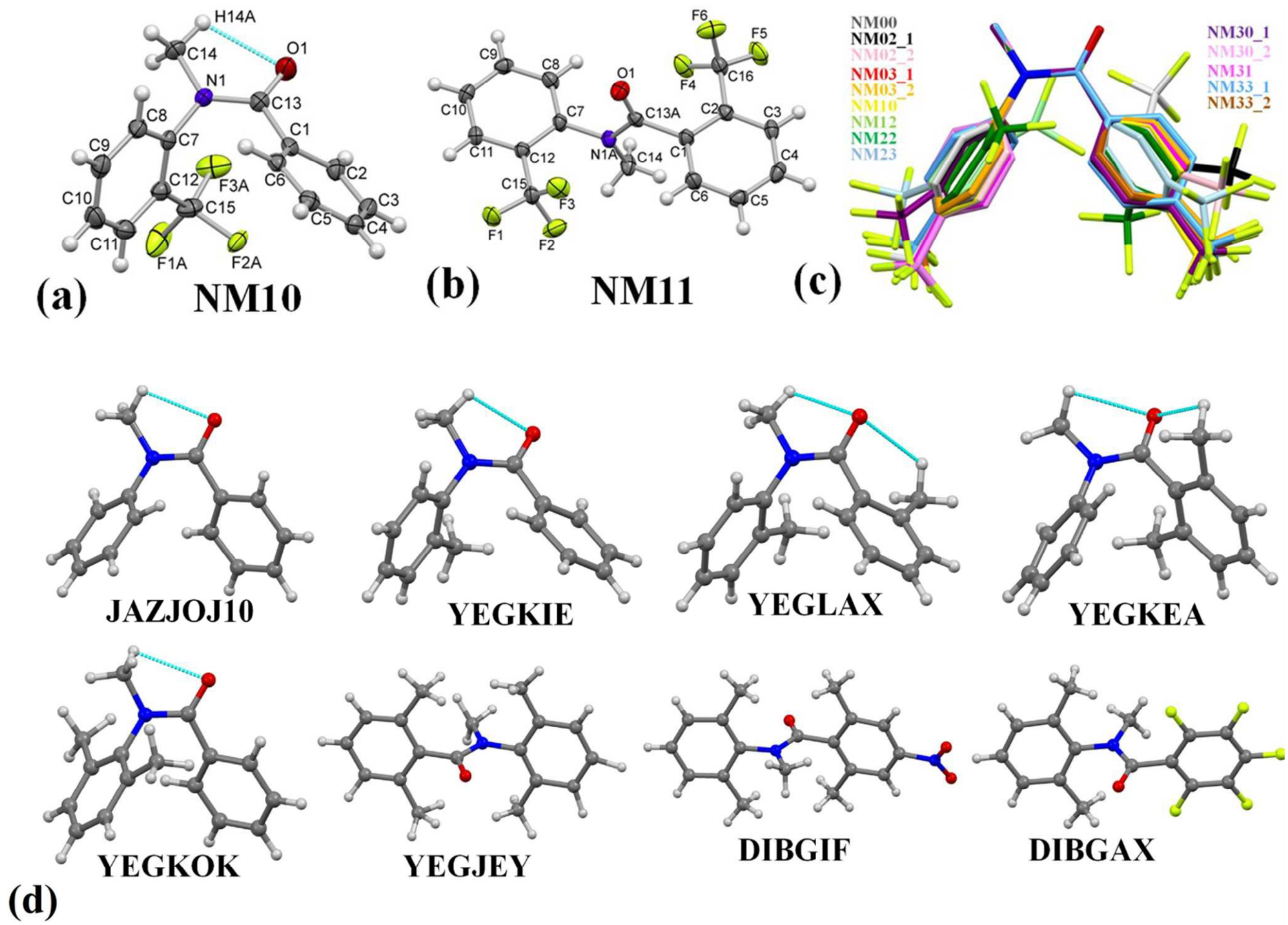

Figure 1(a) – (b): *ORTEP* of **NM10** and **NM11** drawn with 50% ellipsoidal probability with atom numbering scheme displaying two possible conformations in this class of compounds. Similar numbering scheme was followed in all the structures. Only the major component of the disordered part of the molecule has been shown for clarity. The dotted lines indicates the presence of an intramolecular C(sp^3)-H···O=C hydrogen bond. *ORTEP* of other molecules are shown in **Figure S5** in ESI. **(c)** Overlay of all the structures in *cis*-geometry, drawn with Mercury 3.0. **(d)** Molecular diagram of related molecules reported in CSD with their reference code. Dotted lines indicate the presence of an intramolecular C-H···O=C hydrogen bond.

Results and Discussion:

ORTEP of **NM10** and **NM11** are presented in **Fig. 1(a) & 1(b)** with the atom numbering scheme. The *ORTEP's* for the remaining compounds are deposited in ESI [**Fig. S5 (a)-(j)]**. The Cambridge Structural Database search (CSD version 5.35 updates Nov 2013) has been performed for related structures to compare the molecular conformation and crystal packing of related molecules with the present series of compounds. The result gave only 8 hits [**Fig. 1(d)**]. The crystal structure of *N*-methyl-*N*-phenylbenzamide (labeled as '**NM00**') is reported (ref code: **JAZJOJ10**) in the CSD. The compounds in this series exist preferably in the *cis*-conformation [**Fig. 1(c)**]. Due to the presence (or substitution of H by a functional group) *ortho* to both the phenyl rings, the conformation may change to *trans* orientation on account of the role of sterics, as is observed in the case of **NM11**, YEGJEY, DIBGIF, DIBGAX. It is of interest to note that the methyl substitution *ortho* to both of the phenyl rings (YEGLAX), exhibits *cis* conformation while substitution by a trifluoromethyl (-CF_3) group at the same position in **NM11** leads to *trans* geometry [**Fig. 1(b)** & **1(d)**]. The reason for this observation may be the possibility of the formation of two intramolecular weak C(sp^3)-H···O=C hydrogen bonds in case of YEGLAX, which stabilizes the molecular conformation in the *cis* geometry. The dihedral angles between the planes formed by the two phenyl rings and the central part (O=C-N-CH_3) of the molecules for all the structures were compared in Table **2** and **3**. The angle between the two phenyl rings for the molecule having *cis*-geometry displays similar value (angle 1, value more than 60°, **Table 2 & 3**). The deviation of phenyl ring (plane 2) on nitrogen side (angle 3, the value being more than 56°) from O=C-N-CH_3 plane (plane 3) was observed to be more than the angle 2 (the value being less than 60° in most cases) which is the dihedral angle between plane 1(phenyl ring on carbonyl side) and plane 3. No significant changes were observed between solid state geometry and gaseous state geometry. The molecular conformation were observed to be stabilized by the presence of an intramolecular weak C(sp^3)-H···O=C hydrogen bond in both the solid state and the gas phase. In case of molecules having the *trans* conformation, both the phenyl rings were nearly orthogonal to the central plane 3 (O=C-N-CH_3 plane) in both the solid state and gas phase geometry to minimize the sterics in the molecule.

From lattice energy calculations, using the PIXEL method, for all the molecules (**Table 4**), it was observed that the values lie between 102 kJ/mol and 115 kJ/mol with the dispersion energy being the major component. Lattice energy of four related molecules in CSD was also calculated from the PIXEL method (**Table 4**). The result demonstrates that the substitution of the methyl group on *N*-methyl-*N*-phenyl benzamide does not exhibit significant changes in the lattice energy.

Molecular pairs and crystal packing analysis

It is of interest to analyze the crystal packing of *N*-methyl-*N*-phenyl benzamides (**NM00**) and compare with that of its trifluoromethyl substituted analogues (**Table 1**) in this study. The molecular pairs extracted from the crystal packing of **NM00** are shown in **Figure 2(a)** along with the associated interaction energies. The analysis of the molecular pairs revealed that the crystal packing in **NM00** is mainly stabilized by the presence of weak C-H···O=C and C-H···π hydrogen bonds [**Fig. 2(a)**, **Table 5**]. The most stabilized motif **I** (I.E = -24.5 kJ/mol) consists of a short C-H···O=C and a C-H···π hydrogen bond resulting in the formation of a molecular chain with the utilization of *b*-glide plane perpendicular to the crystallographic *a*-axis [Fig. 2(b)]. Such chains are interconnected with the second most stabilized molecular motif **II** (I.E = -19.6 kJ/mol) which consist of a pair of C-H···π hydrogen bond and a short H···H contact. The important fact observed here is that the motif **I**, which consists of a short C-H···O hydrogen bond ($d_{H\cdots O}$ = 2.41Å), has 34% electrostatic (coulombic + polarization) and 66% dispersion contribution out of the total stabilization while these values corresponding to motif **II** are 22% and 78% respectively, which primarily involves C-H···π hydrogen bonds. Similar trends were observed in other motifs as well. Motifs which involve C-H···π hydrogen bonds (**III**, **VI, VII**), displays a dispersion contribution greater than 72%, the highest being in case of motif **VI** (97%) wherein no interactions less than the sum of the van der Waals radii [66] were observed. Furthermore, in case of motifs **IV** and **V**, where weak C-H···O hydrogen bonds are present, the dispersion contribution decreases to 62%. The motif **IV** was observed to be utilized in the formation of a molecular chain along *c*-axis (using *c*-glide plane perpendicular to *a*-axis) and such chains are interconnected with motifs **V** and **VI [Fig 2(c)]**.

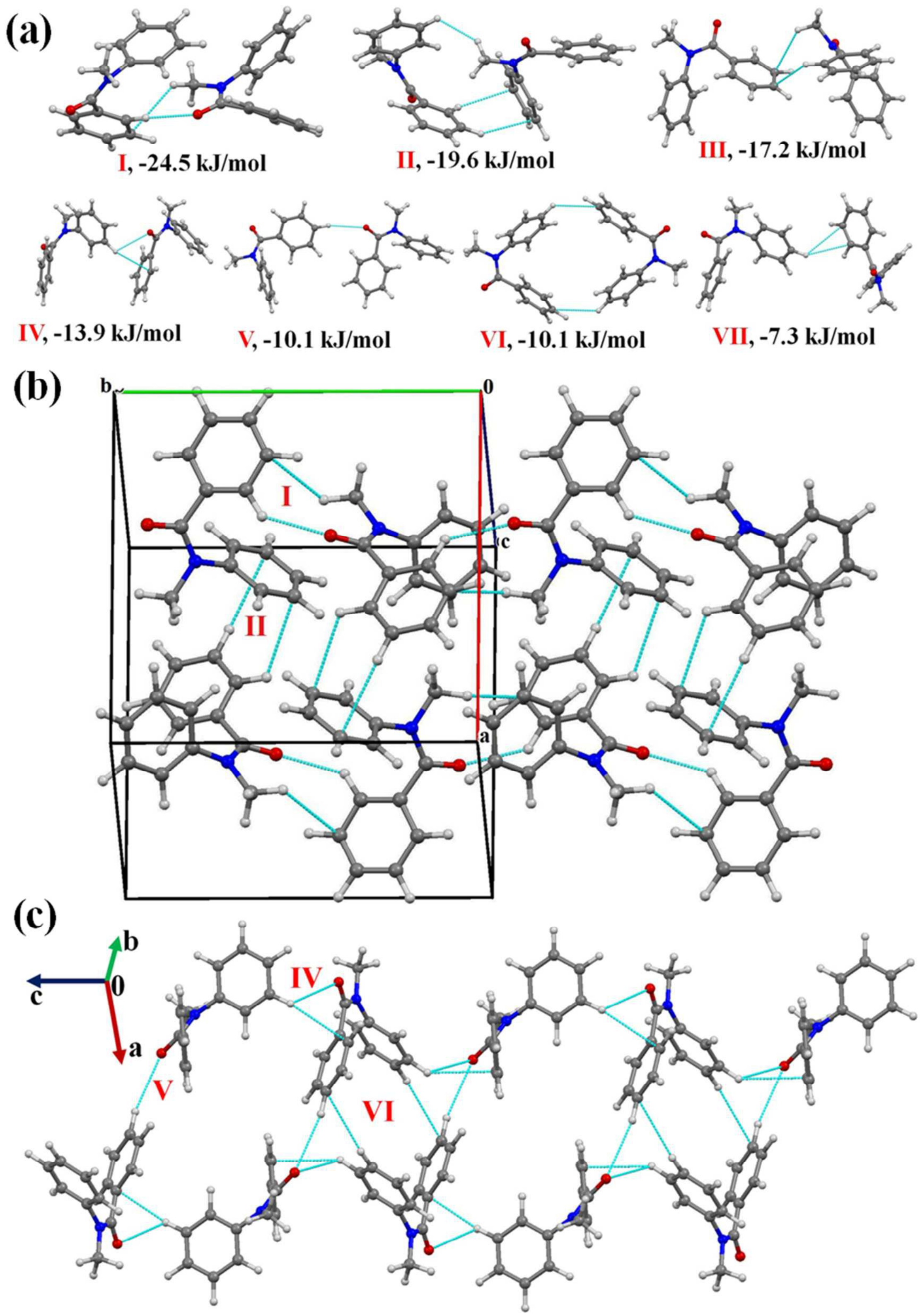

Figure 2(a): Selected molecular pairs along with their PIXEL interaction energy in **NM00**. Roman numbers in red indicate the molecular pairs (in **Table 5**). **(b)** Packing of molecules *via* the utilization of weak C-H···O=C and C-H···π hydrogen bonds in **NM00**. The molecular pairs in **Table 5** were indicated with Roman numbers in red in all figures in this study. **(c)** Weak C-H···O=C and C-H···π hydrogen bonds in the packing of molecules in **NM00** along the crystallographic *c*-axis.

N-methyl-N-phenyl-3-(trifluoromethyl)benzamide (NM02)

The compound **NM02** crystallizes in the monoclinic centrosymmetric *C*2/*c* space group with two molecules in the asymmetric unit. The asymmetric unit (motif **V**, I.E = -22.4 kJ/mol, **Table 5**) is held *via* a short C(sp^2)-H···O=C (2.45Å/141°; involving acidic hydrogen, H2′) and a short *type II* C(sp^3)-F···F-C(sp^3) contact [2.823(2)Å, 98(1)°, 158(1)°]. The presence of a σ-hole on the fluorine atoms in the CF_3 group has recently been revealed, which is responsible for the formation of such interactions in the crystal packing [36]. It was also well established that the *type II* halogen-halogen contacts may be consider as a halogen bond [67-68]. It is to be noted here that the electrostatic contribution (coulombic + polarization) towards the total stabilization energy is 32%, between the two interacting molecules in the asymmetric unit.

Furthermore, the analysis of the molecular pairs extracted [**Fig. 3(a)**] from the crystal packing of **NM02**, revealed that amongst the top six most stabilized motifs, five consists (motif **I, III - VI**) of the presence of weak C-H···O=C hydrogen bonds with stabilization energy ranging from 17.6 kJ/mol to 35.1 kJ/mol with substantial electrostatic contributions (in the range of 31 to 45%, **Table 5**). The highest stabilized (with 43% electrostatic contribution) molecular motif **I** involves the presence of dimeric bifurcated weak C-H···O=C hydrogen bonds with donor atoms from two different C-H bonds[C(sp^2)-H and C(sp^3)-H] in different electronic environment. The motif **II**, **III** and **IV** were observed to provide similar stabilization (I.E being -31.5, -31.1 and -30.0 kJ/mol respectively) but differing in the nature of the participating interactions. In case of motif **II**, the molecules interact *via* the existence of C-H···π hydrogen bonds and π···π interactions, the % contribution from the dispersion being the highest (77%) amongst all. The motif **III** involves one short C(sp^2)-H···O=C (2.46Å/144°) and two C(sp^2)-H···F-C(sp^3) hydrogen bonds (2.43Å/138°; 2.65Å /126°), the former being significantly short. The dispersion contribution is 59% and this is a significant contribution and comparable to related weak H-bonds,. Furthermore, motif **IV**, which involves one C(sp^2)-H···O=C and a short C-H···π hydrogen bond (2.65Å/157°, **Table 5**) shows the dispersion contribution (69%) in between that of motif **II** and **III**. Two bifurcated C(sp^2)-H···O=C along with a C(sp^3)-H···F-C(sp^3) were observed to hold the molecules in motif **VI** (I.E = -18.2 kJ/mol) with the highest (45%) electrostatic contribution amongst all the motifs. Further, in case of motif **VII** (I.E = -14.7 kJ/mol) and **VIII** (I.E = -14.5 kJ/mol), where C-H···π hydrogen bonds and π···π interactions present, the total stabilization is dominated from the contribution due to dispersion interactions (72 and 69% respectively). It is to be noted that the crystal packing in **NM02** was also stabilized, albeit less, by the presence of weak C(sp^2/ sp^3)-H···F-C(sp^3) hydrogen bonds (motif **IX** - **XI**). The motif **IX** (I.E = -10.1 kJ/mol) shows the presence of one bifurcated C(sp^2)-H···F- C(sp^3) and a short and directional C(sp^3)-H···F-C(sp^3) (2.51Å/160°) hydrogen bond with the electrostatic contribution being 41% of the total stabilization. The motif **X** and **XI**, [involving bifurcated C(sp^2)-H···F-C(sp^3) hydrogen bond] which were observed in contributing a similar stabilization (-7.1 and -7.0 kJ/mol) towards the crystal packing, contains 32% contribution from electrostatics. The stabilization energy for a C-H···F hydrogen bond was reported to be -0.40 kcal/mol (-1.6 kJ/mol) by *ab initio* theoretical calculation in the molecular crystal [69]. It was observed in the same work that the stabilization energy for a C-H···F hydrogen bond is mainly dominated by electrostatic and dispersion component with the latter being more prominent. **Figure 3(b)** and **3(c)** display the packing of molecules in **NM02** with the utilization of such weak interactions.

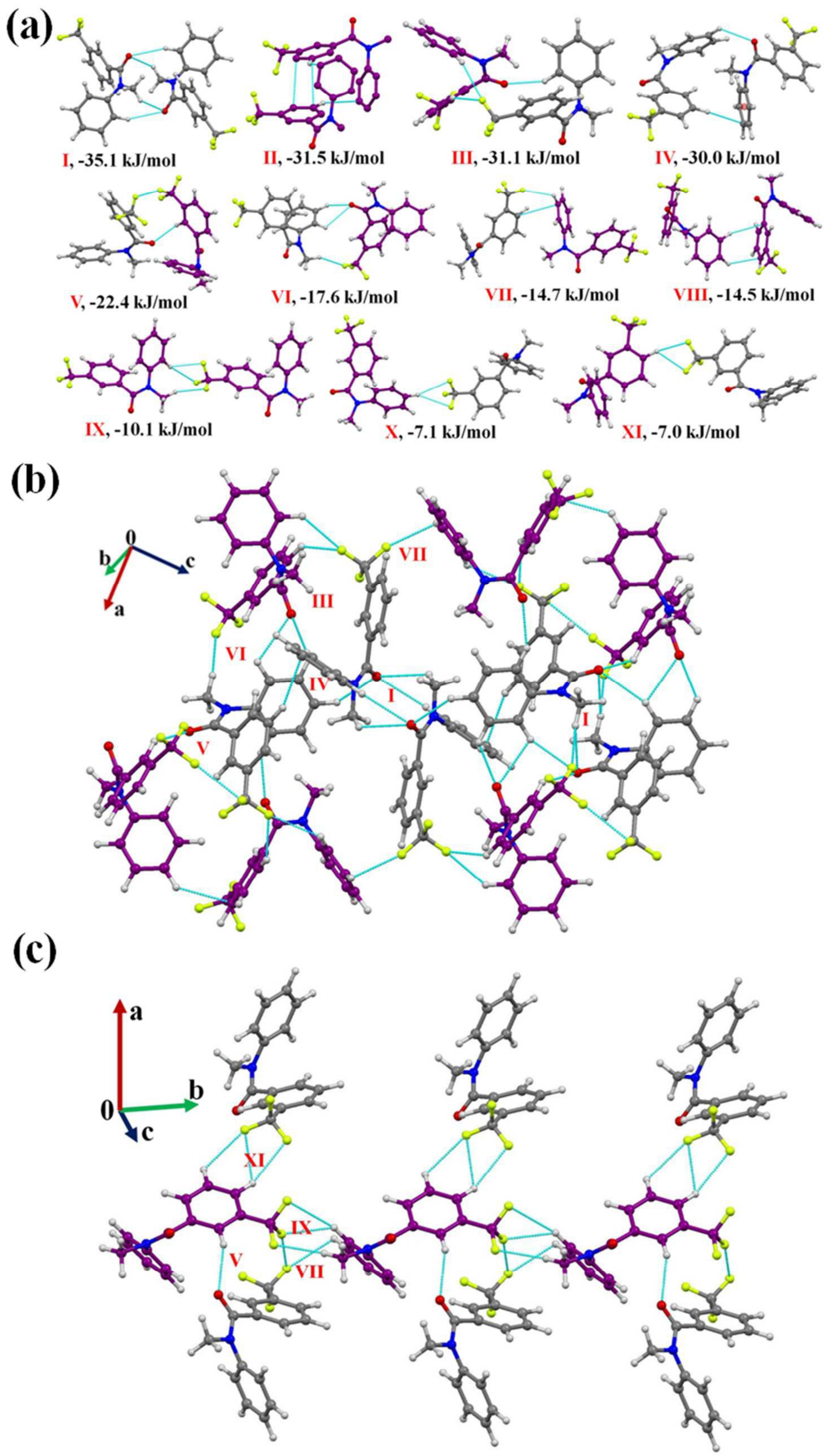
(a)
I, -35.1 kJ/mol
II, -31.5 kJ/mol
III, -31.1 kJ/mol
IV, -30.0 kJ/mol
V, -22.4 kJ/mol
VI, -17.6 kJ/mol
VII, -14.7 kJ/mol
VIII, -14.5 kJ/mol
IX, -10.1 kJ/mol
X, -7.1 kJ/mol
XI, -7.0 kJ/mol
(b)
0
b
c
a
VII
III
VI
IV
I
I
V
(c)
a
b
0
c
XI
IX
V
VII

Figure 3(a): Selected molecular pairs along with their PIXEL interaction energy in **NM02**. C-atoms are in purple and represent the second molecule in the asymmetric unit. **(b)** Packing of molecules in **NM02** with the presence of weak C-H···O=C, C-H···F and C-H···π hydrogen bonds. **(c):** Part of the crystal packing down the *ab* plane in **NM02**, displaying the presence of weak C-H···O=C and C-H···F-C(sp^3) hydrogen bonds along with C(sp^3)-F···F-C(sp^3) interactions.

N-methyl-*N*-phenyl-4-(trifluoromethyl)benzamide (NM03)

The compound **NM03** crystallizes in the monoclinic centrosymmetric $P2_1/c$ space group with Z′ = 2. A bifurcated weak C(sp^3)/(sp^2)-H···O=C hydrogen bond [this includes a short and highly directional C(sp^2)-H···O=C; 2.26Å, 161°, **Table 5**] along with π···π interactions were observed to link the molecules in the asymmetric unit. This molecular motif has the highest stability [motif **I**, I.E = -39.3 kJ/mol, **Fig. 4(a)**] in the crystal packing of **NM03** [**Fig. 4(b)** &**(c)**] with the electrostatic contribution being 43%. Although motif **I** primarily consists of π···π interactions, a relatively high electrostatic contribution towards the total stabilization (in comparison to related molecular motifs where C-H···π or π···π present, the electrostatic contribution were observed to be less than 30%) is due to the presence of short C(sp^3)/(sp^2)-H···O=C hydrogen bonds. Similarly, in case of the second most stabilized molecular pair (motif **II**, I.E = -35.1 kJ/mol) where molecules are linked with a short C(sp^2)-H···O=C (2.45Å, 139°) and two (including one at short distance) directional C(sp^2)-H···π (2.49 Å, 159°; 2.80Å, 154°) hydrogen bonds, the electrostatic contribution being 35% [**Table 5**]. It is to be noted here that the motif **I** [consist of highly short and directional C(sp^2)-H···O] has approximately 6 kJ/mole more coulombic contribution than that in motif **II** while the opposite situation were observed in case of dispersion contribution with similar magnitude of approximately 6 kJ/mole**.** The motif **III** (I.E = -27.6 kJ/mol) and **IV** (I.E = -23.6 kJ/mol) are characterized by the presence of weak C(sp^2)-H···π and π···π interactions, the dispersion energy contribution exceeds to 75% and 70% respectively. Further, a short and highly directional C(sp^2)-H···O hydrogen bond (2.33Å, 173°, motif **V**) was observed to provide 20.3 kJ/mol stabilization towards the crystal packing in **NM03**, the contribution from electrostatics being 42%. Similar trends was observed in case of motifs **VI** and **VII** [**Fig. 4(a)**] where molecules are held *via* the presence of C(sp^2)-H···O hydrogen bonds along with the other interactions (**Table 5**). Moreover, the packing of molecules in **NM03** were also observed to be stabilized by the presence of weak C(sp^2)-H···F-C(sp^3) hydrogen bonds (motifs **VIII** – **XII** except **X**, which consist of long C(sp^2)-H···O (2.96Å/ 159°) with stabilization energy ranging from 9.2 kJ/mol to 5.6 kJ/mol with $\%E_{elec}$ in the range between 27% to 46% (**Table 5**). **Figure 4(c)** shows that the highly stabilized motif **I** and **III** are interlinked *via* the presence of weak C(sp^2)-H···F-C(sp^3) hydrogen bonds down the (110) plane in the molecular packing of **NM03**.

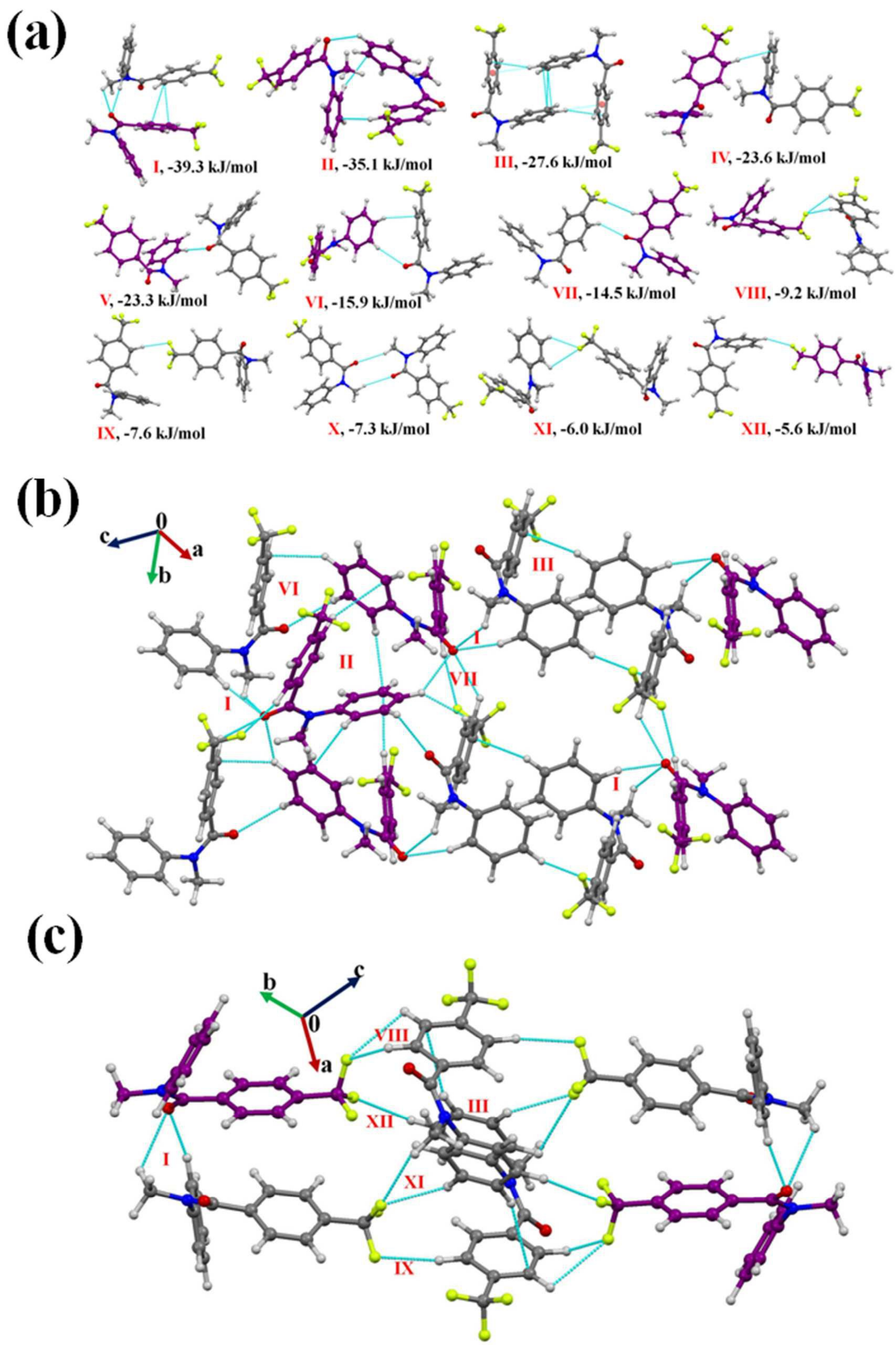
(a)
I, -39.3 kJ/mol
II, -35.1 kJ/mol
III, -27.6 kJ/mol
IV, -23.6 kJ/mol
V, -23.3 kJ/mol
VI, -15.9 kJ/mol
VII, -14.5 kJ/mol
VIII, -9.2 kJ/mol
IX, -7.6 kJ/mol
X, -7.3 kJ/mol
XI, -6.0 kJ/mol
XII, -5.6 kJ/mol
(b)
c
0
a
b
VI
III
II
I
VII
I
I
(c)
b
c
0
a
VIII
XII
III
I
XI
IX

Figure 4(a): Selected molecular pairs along with their PIXEL interaction energy in **NM03**. C-atoms are in purple and represent the second molecule in the asymmetric unit. **(b)** Packing of molecules down the (101) plane in **NM03**, displaying the presence of weak C-H···O=C, C-H···π and C-H···F-C(sp^3) hydrogen bonds. **(c)** Part of the crystal packing displaying the motifs **I** and **III** (**Table 5**) connected *via* weak C(sp^2)-H···F-C(sp^3) hydrogen bonds down the (110) plane in **NM03**.

***N*-methyl-*N*-(2-(trifluoromethyl)phenyl)benzamide (NM10):**

The compound **NM10** crystallizes in the orthorhombic centrosymmetric *Pbca* space group with Z = 8. Molecular pairs extracted from the crystal packing in **NM10** have been highlighted [**Figure 5(a)**] alongwith their interaction energies. The highest stabilized molecular motif **I** (I.E = -36.2 kJ/mol) is similar to motif **II** in **NM02** and motif **III** in **NM03** [**Fig 5(a)**]. As in the previous case, molecules are linked *via* the presence of a short C-H···π with %E_{disp} = 60 which is 15-17% less than the previous case (**Table 5**). This may be due to the absence of C···C (π···π) interaction, in the present case, at a distance less than 4Å. It is observed, on viewing down the crystallographic *bc* plane [**Fig. 5(b)**], that the molecular chains formed with the utilization of motif **III** (I.E = -20.6 kJ/mol) and motif **VI** (I.E = -9.6 kJ/mol) along the *b*-axis are interconnected with motif **II** (I.E = -28.1 kJ/mol) and **V** (I.E = -11.7 kJ/mol). The motif **II**, consists of a short C(sp^3)-H···O=C (2.59Å, 130°) and C(sp^2)-H···π at longer distances [%E_{disp} being 65%]. Further, the motif **III** and **IV**, which involves weak C-H···F-C(sp^3) hydrogen bonds at a distance greater than the sum of the van der Waals radii of H and F (2.67Å), were observed to provide more stabilization in comparison to motif **V** and **VI** which consists of a short C(sp^2)-H···O=C hydrogen bond (**Table 5**). The differences amongst them appear in the nature of the individual components of the total stabilization energy. In case of **III** and **IV** it is of dispersive origin (more than 62%) while motif **V** (% E_{elec} = 50) and motif **VI** (% E_{elec} = 45) shows a very significant contribution from electrostatics. In the crystal packing of **NM10**, a less stabilized molecular motif (motif **VII**, -6.9 kJ/mol), involving weak C(sp^2)-H···π hydrogen bond, were also observed with %E_{disp} = 84.

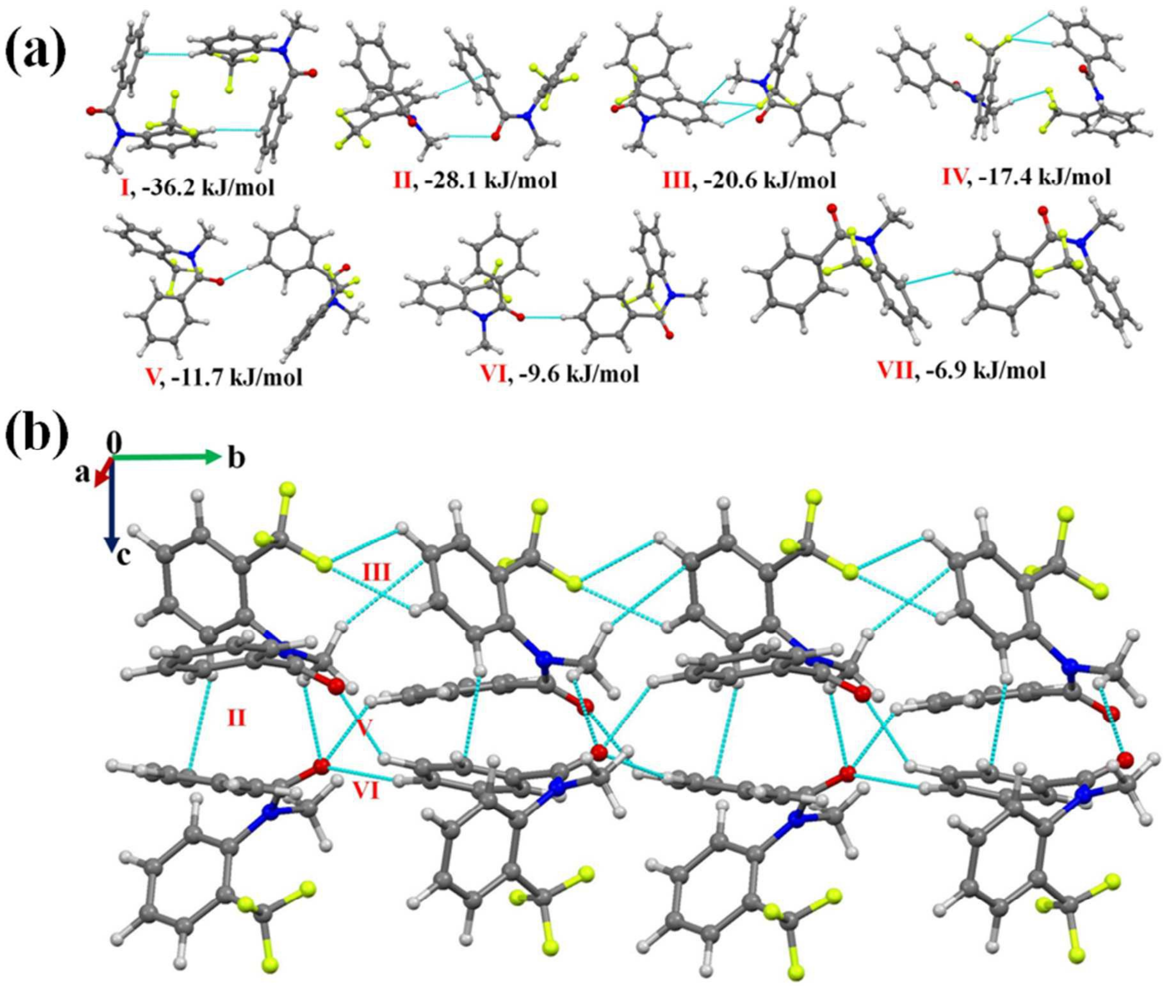

Figure 5(a) Molecular pairs along with their interaction energy extracted from the crystal packing in **NM10. (b)** Packing of molecules down the *bc* plane *via* weak C-H···O=C, C-H···π and C-H···F-C(sp^3) hydrogen bonds in **NM10.**

***N*-methyl-*N*-(4-(trifluoromethyl)phenyl)benzamide (NM30):**

The compound **NM30** crystallizes in the centrosymmetric monoclinic space group $P2_1/c$ with two molecules in the asymmetric unit. The asymmetric unit was observed to be a highly stabilized molecular pair (I.E = -25.6 kJ/mol with % E disp = 65) in the crystal packing involving weak C(sp^2)-H···O=C and C(sp^2)-H···π hydrogen bond alongwith the presence of a π···π interaction. The molecular motifs **II** to **V** were observed to provide similar stabilization (**Table 5**, I.E being approximately 18.2 to 18.8 kJ/mol) towards the crystal packing. Amongst these, motifs **II** and **III** were found to be involved in the formation of a short C(sp^2)-H···O=C hydrogen bond (2.53Å, 133°; 2.49Å, 136°) with an electrostatic contribution of 41% and 42% respectively. The motifs **IV** and **V** were involved in the formation of a weak C(sp^2)-H···F along with the π···π interaction, hence shows a high dispersion contribution (77 and 76% in the two cases). The weak C(sp^2)-H···π hydrogen bond along with the π···π interactions were observed to connect to two symmetry independent molecules in the crystal packing in motif **VI** (I.E = -17.0kJ/mol with $\%E_{disp}$ being 74). Moreover, the dimeric C(sp^3)-F···π interaction was found to link two molecules in the crystal packing, motif **VII** (I.E = -17.0 kJ/mol) and **VIII** of similar stabilization (**Table 5**) with substantial dispersion contribution (more than 70%). The interaction energy of the C(sp^3)-F···π interaction (for one interaction, the approximate value will be -8.5kJ/mol; here a phenyl group, involved in the interaction, is attached with an electron withdrawing $-CF_3$ group) is similar to the value for the C-F···π_F interaction (-2.43kcal/mol, interaction of fluoromethane with hexafluorobenzene) by MP2/aug-cc-pVDZ calculation [70]. In the motif **IX** and **X** (I.E being -16.0 and 15.5 kJ/mol respectively), a weak C(sp^2)-H···F hydrogen bond along with C(sp^3)-F···C=O interaction were observed to connect the molecules. Furthermore, weak C(sp^2)-H···O=C and C(sp^3)-H···F-C(sp^3) hydrogen bonds were observed to be involved in two similarly stabilized molecular pairs (Motif **XI** and **XII**) in the crystal packing. A short and directional C(sp^2)-H···π (2.73Å, 152°) along with weak C(sp^2)-H···O=C hydrogen bonds were recognized to involve in connecting the two symmetry independent molecules in the crystal packing in motif **XIII** (I.E = -12.6 kJ/mol with $\%E_{disp}$ = 63%). Moreover, *type I* C(sp^3)-F···F-C(sp^3) interactions were observed to connect the molecules in the weakly stabilized molecular motif **XIV** and **XV** with a positive coulombic contribution. The stabilization in these motifs is mainly of dispersion origin (more than 94%, **Table 5**) with overall stabilization energy being 1.8 kJ/mol. This stabilization energy is comparable with the value reported in a recent analysis (by *ab initio* method and Symmetry-Adapted Perturbation Theory (SAPT)) on the nature of C-F···F-C for the all unique dimers, extracted from the crystal structure of CF_4, C_2F_4 and C_6F_6 [71]. From the SAPT analysis, it was observed that the total stabilization energy was mainly dominated by the dispersion energy component and the electrostatic component can be stabilizing or destabilizing depending on the orientation of the interacting dimers. **Figure 6(b)** represents the packing of molecules in **NM30** down the crystallographic *ac* plane.

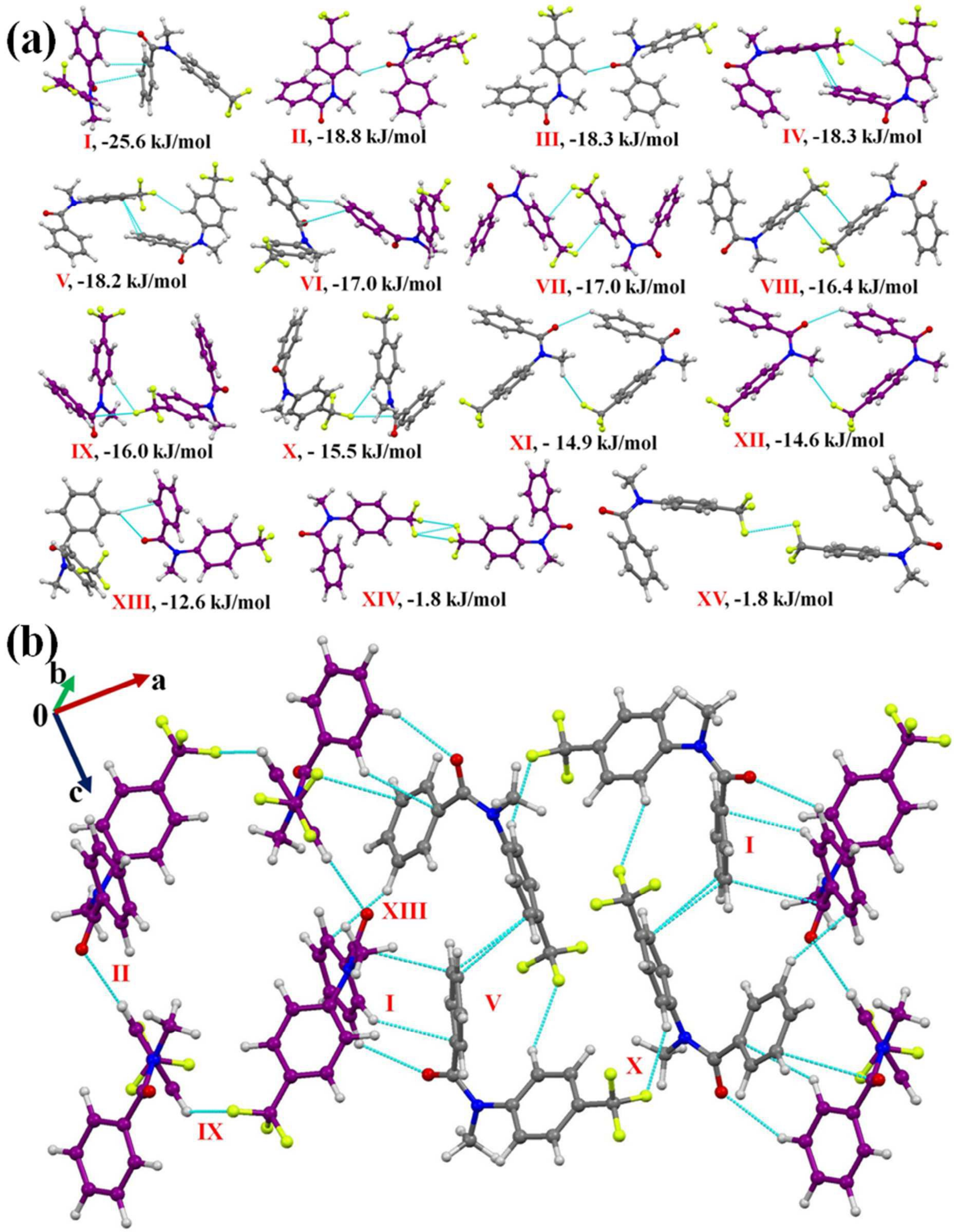

Figure 6(a): Selected molecular pairs in **NM30** along with their interaction energies. **(b)** Packing of molecules down the *ac* plane *via* weak C(sp^2)-H···O=C, C(sp^2) -H···F-C(sp^3), C(sp^2)-H···π hydrogen bonds and π···π interactions in **NM30.**

***N*-methyl-2-(trifluoromethyl)-*N*-(2-(trifluoromethyl)phenyl)benzamide (NM11):**

The compound **NM11** crystallizes in a centrosymmetric monoclinic space group $P2_1/c$ with Z = 4. Unlike other molecules in this series, the molecular structure is observed to be in *trans* conformation with C=O and N-C bond oriented opposite to each other. This may be due to the minimization of the steric effect, when two CF_3 groups are present at the *ortho* position of the two phenyl rings in the molecule. The (CH_3)N-CO was observed to be disordered at two positions with the occupancy ratio 0.939(3): 0.061(3), [modeled with PART command in the SHELXL 2013 at two orientations 'A' (for higher occupancy) and 'B']. Selected molecular pairs extracted from the crystal packing have been given in **Figure 7(a)**. A dimeric molecular motif, consists of a pair of short and directional C(sp^2)-H···O=C (2.46Å, 160°) and C(sp^2)-H···F-C(sp^3) (2.49Å, 144°) hydrogen bonds along with offset π···π stacking interactions (motif **I**, I.E = -40.8 kJ/mol), was observed to provide highest stabilization towards the crystal packing. It is to be noted here that the % E_{elec} contribution was 54 % with the coulombic contribution of 42%. The next two stabilized motifs were (**II** and **III**) involving the formation of π···π stacking interactions between pair of molecules, the I.E being -22.0 and -17.8 kJ/mol respectively with stabilization being mainly dispersive in origin. It was observed that with increase in the interacting distance of the Ph-ring (from motif **II** to motif **III)**, the dispersion contribution towards the total stabilization increased from 74% to 94% with no stabilization from coulombic (positive coulombic contribution, **Table 5**) in case of the latter. Further, motifs **IV** and **V** were observed to contribute similar stabilization towards the crystal packing (-16.7 kJ/mol and -16.6 kJ/mol) but different in the nature of the involved interactions. The motif **IV** appeared to engage *via* long C(sp^2)-H···F-C(sp^3) hydrogen bond with %Eelec being 26% while in motif **V**, the molecules are connected with short C(sp^2)-H···O=C (2.35Å, 144°) and C(sp^2)-H···F-C(sp^3) (2.65Å, 154°) hydrogen bond. As expected, this results in the increase of the % E_{elec} contribution to 59%, having 45% coulombic contribution (**Table 5**). Packing of molecules in **NM11** was recognized to involve the formation of molecular networks where motif **I** is connected with the motif **V** [**Fig. 7(b)**]. Moreover, the motif **VI** [consisting of the pair of weak C(sp^3)-H···F-C(sp^3) and a C-H···π hydrogen bonds at distances longer than the sum of van der Waals radii of the involved atoms, I.E = -15.8 kJ/mol, %E_{disp} = 93%] generate a molecular chain with the utilization of 2_1-screw along the *b*-axis [**Fig 7(c)**]. Such a chain was observed to be linked *via* weakly stabilized molecular motif **VII** (I.E = 5.3 kJ/mol, $\%E_{disp}$ = 69%) down the *bc* plane which involves two weak C(sp^2)-H···F-C(sp^3) (2.58Å, 156°; 2.78Å, 147°) hydrogen bonds (**Table 5**).

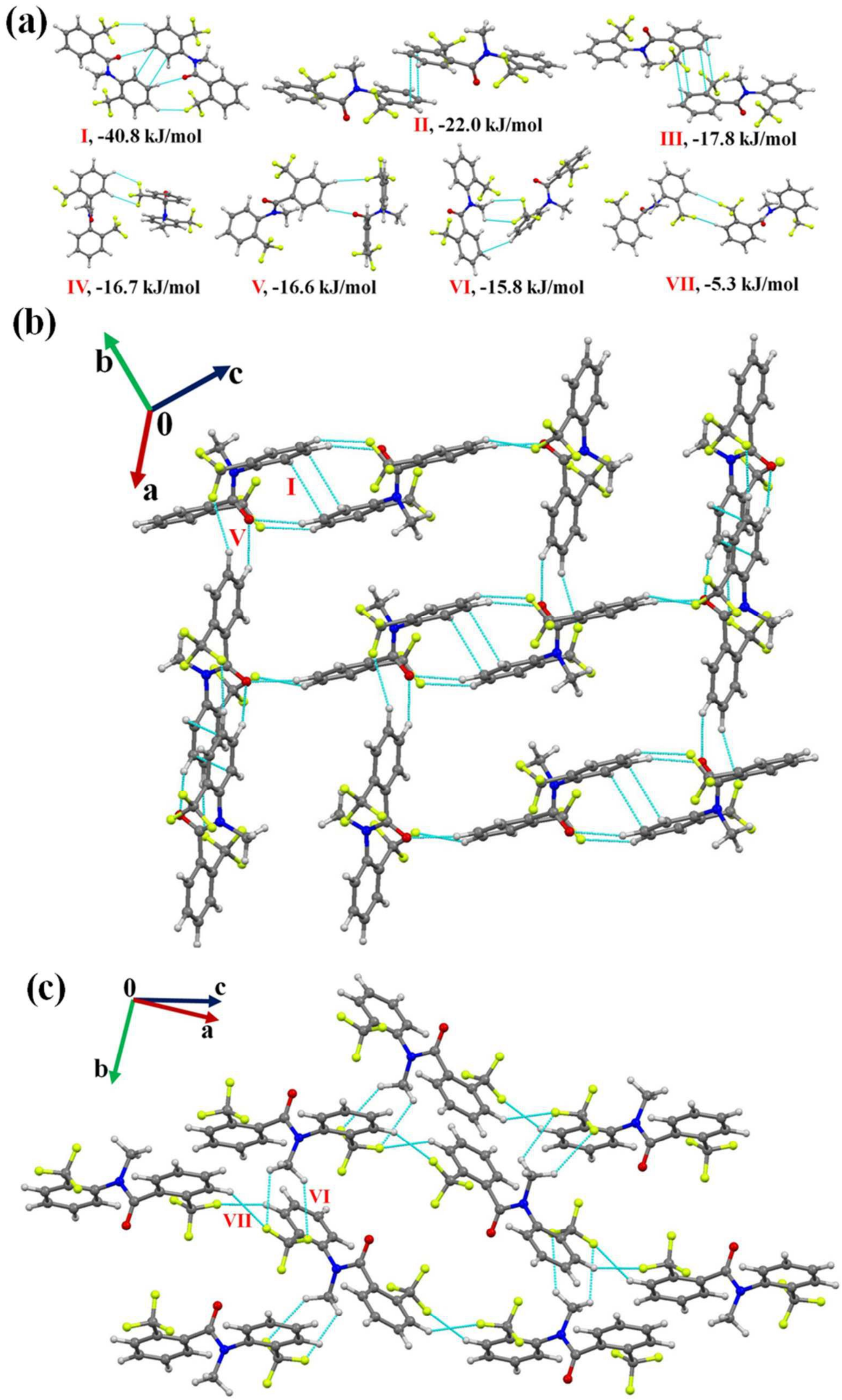
(a)
I, -40.8 kJ/mol
II, -22.0 kJ/mol
III, -17.8 kJ/mol
IV, -16.7 kJ/mol
V, -16.6 kJ/mol
VI, -15.8 kJ/mol
VII, -5.3 kJ/mol
(b)
b
c
0
a
I
V
(c)
0
c
a
b
VI
VII

Figure 7(a): Selected molecular pairs extracted from the crystal packing in **NM11** along with their interaction energies. **(b)** Molecular network formed with the utilization of weak C(sp^2)-H···O=C, C(sp^2) -H···F-C(sp^3) hydrogen bonds and π···π interactions in **NM11. (c):** Packing of molecules *via* C(sp^2)/(sp^3)-H···F-C(sp^3) hydrogen bonds in **NM11**.

***N*-methyl-3-(trifluoromethyl)-*N*-(2-(trifluoromethyl)phenyl)benzamide (NM12):**

The compound **NM12** crystallizes in the monoclinic $P2_1/c$ space group with Z = 4. The analysis of the molecular pairs extracted from the crystal packing [**Fig. 8(a)**] shows that the highest stabilized molecular motif **I** [-36.2 kJ/mol with $\%E_{disp}$ = 80%; involves C(sp^2) -H···π hydrogen bonds and π···π interactions] appears to be a robust motif in this series of compounds as also previously recognized in **NM02**, **NM03**, **NM10**. But it is also to be noted here that this was not observed in the molecular packing of **NM00**. The packing of molecules down the *bc* plane in **NM12** displays the formation of a molecular chain along the crystallographic *c*-axis *via* motif **III** (I.E = 22.3 kJ/mol) which was observed to be interlinked with motif **II** (I.E = -25.6 kJ/mol) and motif **V** (I.E = -12.1 kJ/mol) [**Fig. 8(b)**]. The motif **II** consists of two short and directional C(sp^2)-H···O=C hydrogen bonds (2.32Å, 160°; 2.57Å, 153°) with 48% contribution from electrostatics (**Table 5**). In case of motif **III** (I.E = -25.6 kJ/mol; $\%E_{elec}$ = 41), a weak C(sp^2)-H···O=C along with a C(sp^2)-H···F-C(sp^3) hydrogen bond was observed to connect the molecules, displaying slightly less stabilization and electrostatic contribution than motif **II** (**Table 5**). Further, a dimeric C(sp^2)-H···F-C(sp^3) hydrogen bonds (2.63Å, 130°) were recognized to link the molecules in motif **V** (with $\%E_{disp}$ = 75%). Moreover, a weak C(sp^2) -H···π along with a weak C(sp^2)-H···F-C(sp^3) hydrogen bond (2.78Å, 149°) were also observed to stabilize the crystal packing in **NM12** (motif **IV,** -15.8 kJ/mol; $\%E_{disp}$ = 76%). A weakly stabilized molecular pair (motif **VI**, I.E = -3.8) involving weak C(sp^2)-H···F-C(sp^3) hydrogen bonds along with a *type I* C(sp^3)-F···F-C(sp^3) interaction (**Table 5**) were also recognized in the crystal packing.

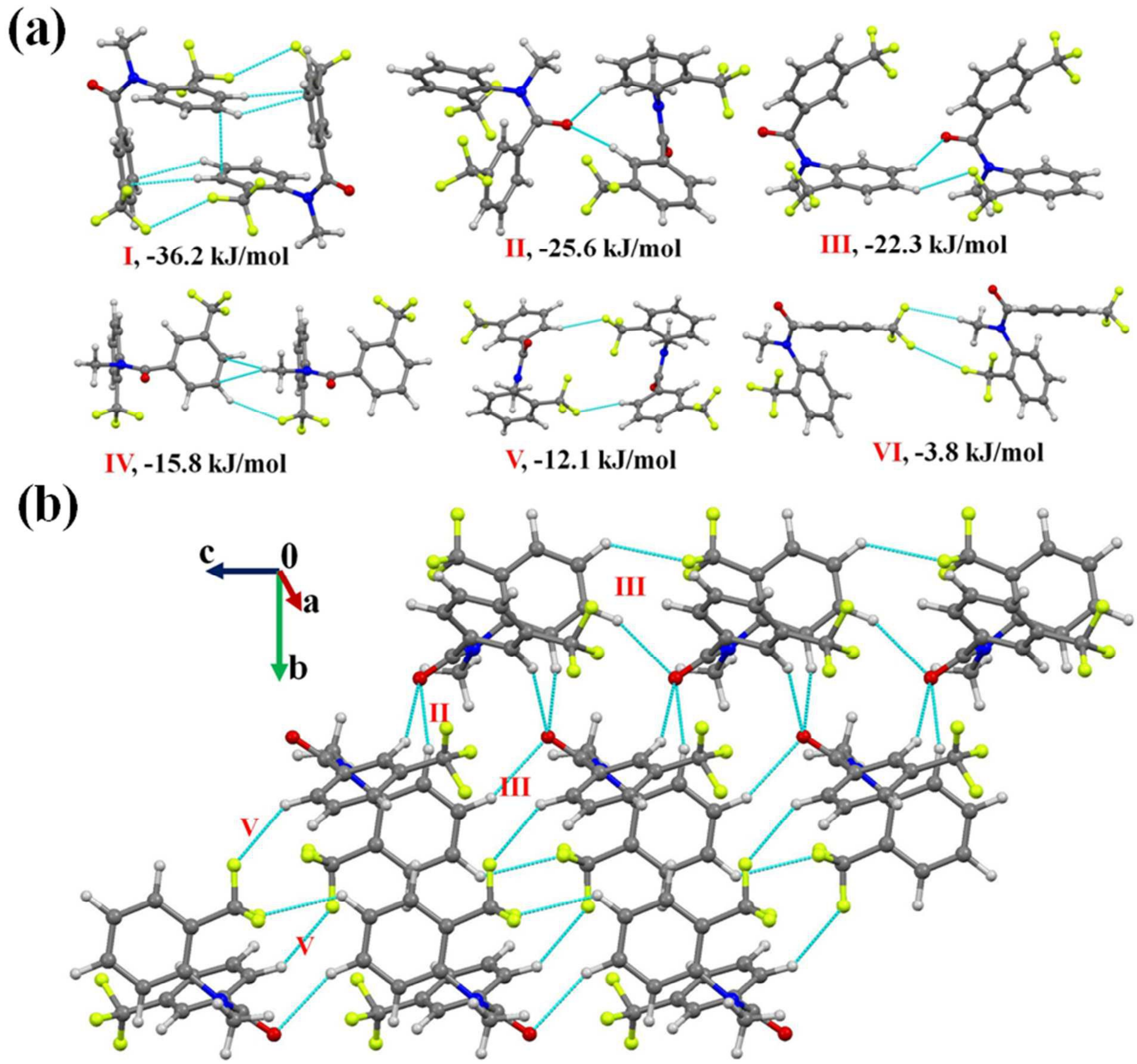

Figure 8(a): Displaying molecular pairs extracted from molecular packing in **NM12.** **(b)** Packing of molecules down the *bc* plane with the utilization of weak C(sp^2)-H···O=C and C(sp^2) -H···F-C(sp^3) hydrogen bonds in **NM12.**

N-methyl-3-(trifluoromethyl)-*N*-(3-(trifluoromethyl)phenyl)benzamide (NM22):

The compound **NM22** crystallizes in the centrosymmetric monoclinic space group ($P2_1/c$) with Z = 4. The molecular pairs, extracted from the crystal packing, are presented in **Figure 9(a)**. Three possible short and/or directional C(sp^2)-H···O=C (2.21Å, 140°; 2.43Å, 173°; 2.69Å, 152°) hydrogen bonds, motif **I,** involving the acidic hydrogen atoms, form the most stabilized (I.E = -37.0 kJ/mol) pair in the crystal packing with the total stabilization being 52% electrostatic (coulombic + polarization) contribution (**Table 5**). Motif **II** (I.E = 26 kJ/mol), being the most common in this series of structures, consists of a weak C(sp^2)-H···π hydrogen bond and π···π interaction, was observed to provide stabilization to the crystal packing, which is primarily of a dispersive (85%) origin. The packing of molecules in **NM22** was observed to form a zig-zag chain *via* motif **I**, with the utilization of *c*-glide perpendicular to the *b*-axis. Such a chain is connected *via* the utilization of motif **III** and **IV** [**Fig. 9(b)**] down the *bc* plane. The motif **III** (I.E = -24.2 kJ/mol) was found to involve a short C(sp^2)-H···π (2.51Å, 148°) along with a weak C(sp^2)-H···F-C(sp^3) hydrogen bond while the motif **IV** (I.E = -15.6 kJ/mol) consists of two C(sp^2)-H···F-C(sp^3) interactions. Both motifs show similar contribution (67%) from dispersion towards the total stabilization. Moreover, a pair of bifurcated weak C(sp^2)-H···F-C(sp^3) hydrogen bonds were also recognized to stabilize (motif **V**, I.E being -10.2kJ/mol) the crystal packing in **NM22**.

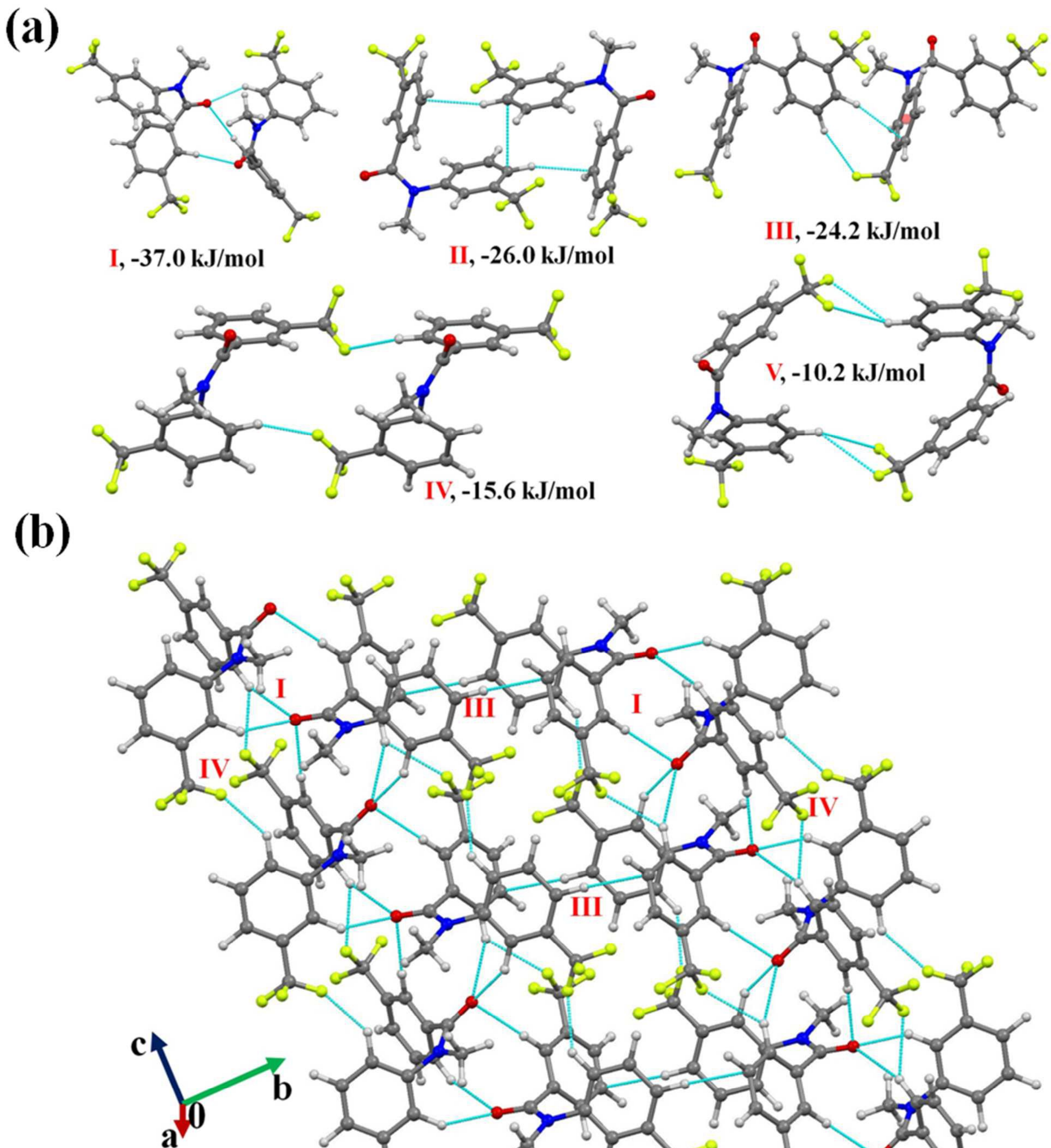

Figure 9(a): Selected molecular pairs extracted from the crystal packing in **NM22**. **(b)** Network of weak C(sp^2)-H···O=C and C(sp^2)-H···F-C(sp^3) hydrogen bonds in the crystal packing down the *bc* plane in **NM22**.

***N*-methyl-4-(trifluoromethyl)-*N*-(3-(trifluoromethyl)phenyl)benzamide (NM23):**

The compound **NM23** crystallizes in the centrosymmetric monoclinic space group ($P2_1/c$) with Z = 4. Molecular pairs, extracted from the crystal packing of **NM23**, along with their stabilization energies are presented in **Figure 10(a)**. The analysis of the results depicts the presence of two similar dimeric stabilizing pairs [motif **I** (observed to be robust in this series) and motif **II**] in the crystal packing. The motif **I** (I.E = -39.1 kJ/mol with %E_{disp} is 71%) was recognized to involve a short C(sp^2)-H···π (2.61Å, 161°) along with the presence of a weak offset π···π stacking interactions while dimeric bifurcated weak C(sp^2)-H···O=C interaction were observed to stabilize (I.E = -38.7 kJ/mol with %E_{disp} reduced to 58%) motif **II** in **NM23 (Table 5)**. Both dimeric motifs **I** and **II** were found to be connected *via* motif **III** and **IV** in the formation of a molecular layer down the *bc* plane [**Fig. 10(b)**]. A bifurcated weak C(sp^2)-H···O=C hydrogen bonds, involving acidic hydrogens, were recognized to link the molecules in motif **III** (I.E = -31.4 kJ/mol, %E_{disp} is 58%) while in case of motif **IV** (I.E = -14.2 kJ/mol with %E_{disp} increased to 73%), a weak C(sp^3)-H···F-C(sp^3) hydrogen bond along with π···π stacking interaction was observed. Furthermore, weak C(sp^2)-H···F-C(sp^3) hydrogen bond along with the *type II* C(sp^3)-F···F-C(sp^3) interaction [in motif **V** (-8.0 kJ/mol) and **VI** (-5.5 kJ/mol)] were also found to stabilize the crystal packing in **NM23** [**Fig. 10(a)**, **Table 5**].

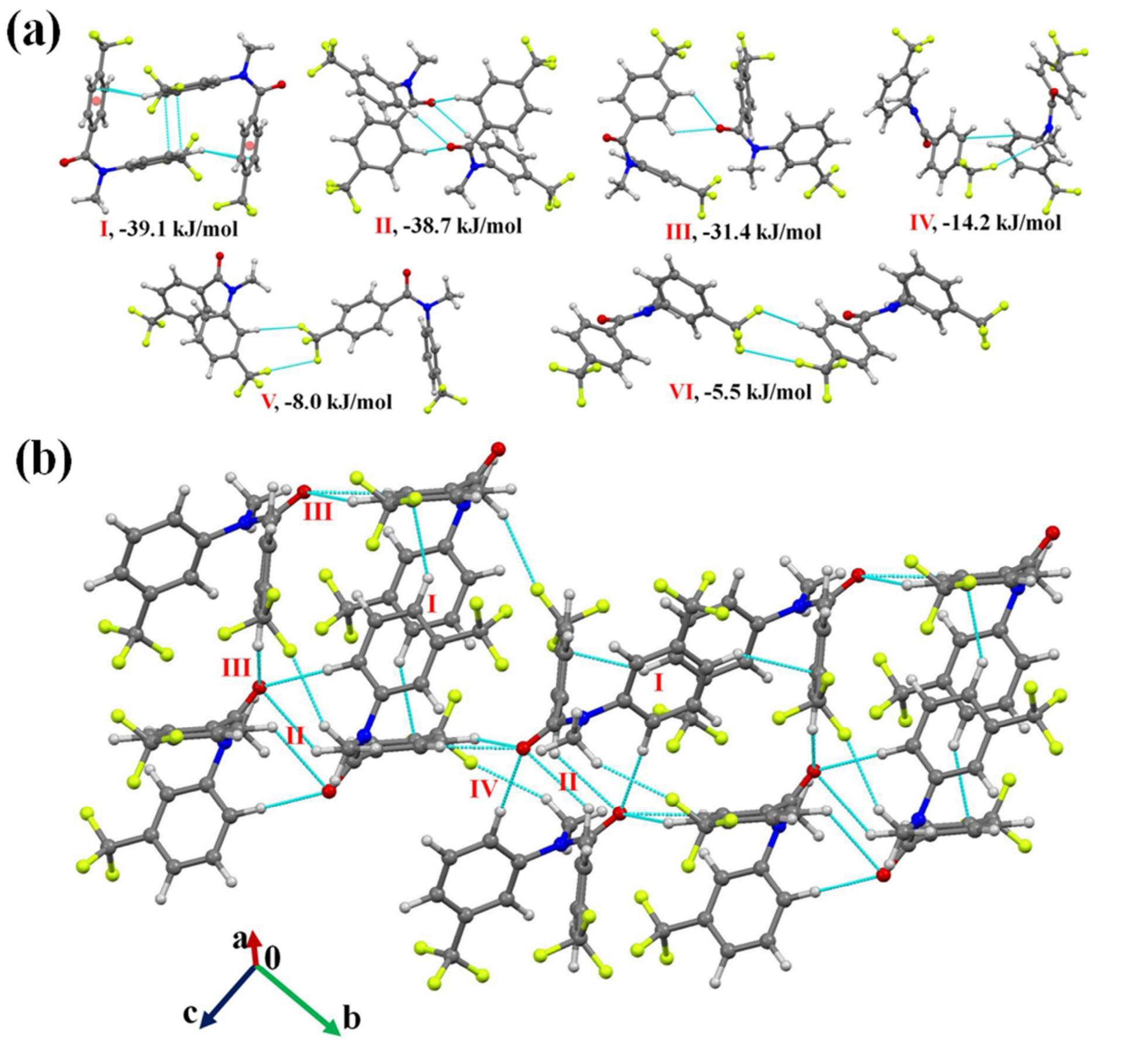

Figure 10(a): Selected molecular pairs along with their interaction energy in **NM23**. **(b)** Packing view down the *bc* plane in **NM23**, depicting network of weak C(sp^2)-H···O=C, C(sp^2)-H···π and C(sp^3)-H···F-C(sp^3) hydrogen bonds.

N-methyl-2-(trifluoromethyl)-*N*-(4-(trifluoromethyl)phenyl)benzamide (NM31):

The compound **NM31** also crystallizes in $P2_1/c$ space group with Z = 4. **Figure 11(a)** depicts the extracted molecular pairs from the crystal packing in **NM31** along with their stabilizing energy. All the molecular motifs were observed to be stabilized by the presence of weak intermolecular interactions. The highest stabilized motif **I** (I.E = -30.1 kJ/mol) was found to involve a short C(sp^2)-H···O=C (2.42Å, 151°) hydrogen bond along with π···π stacking with dispersion contribution being 66%. The motif **I** connects the molecule along the *b*-axis utilizing 2_1-screw in the formation of molecular chains in the crystal packing [**Fig. 11(b)**]. The chain is further stabilized *via* motif **II** (I.E = -22.1 kJ/mol with %E_{disp} being 52%), which involve a short C(sp^2)-H···O=C (2.54Å, 149°) along with a short C(sp^2)-H···F-C(sp^3) (2.38Å, 135°) and a bifurcated weak C(sp^2)/(sp^3)-H···F- C(sp^3) hydrogen bonds. Further, a weak C(sp^2)-H···O=C with support from a bifurcated C(sp^2)-H···F-C(sp^3) hydrogen bond (motif **IV**, -18.2 kJ/mol) was involved in the formation of a molecular chain with the utilization of *c*-glide perpendicular to the *b*-axis. The chain was observed to be connected with motif **I** and motif **III** down the *ac* plane [**Fig 11(c)**]. The motif **III** (I.E = -19.6 kJ/mol with %Edisp = 73%) consists of a dimeric weak C(sp^3)-H···F-C(sp^3) hydrogen bond along with π···π stacking. The packing of molecules in **NM31** was also observed to involve the formation of a molecular motif **V** with weak C(sp^3)-H···π interactions [the stabilization energy is -14.2 kJ/mol]. Furthermore, weakly stabilized molecular motif **VI** [-9.2kJ/mol; involving a dimeric C(sp^2)-H···F- C(sp^3) hydrogen bonds] and motif **VI** [-4.9 kJ/mol; involving C(sp^3)-F···F-C(sp^3) interactions] were also recognized in the crystal packing of **NM31**.

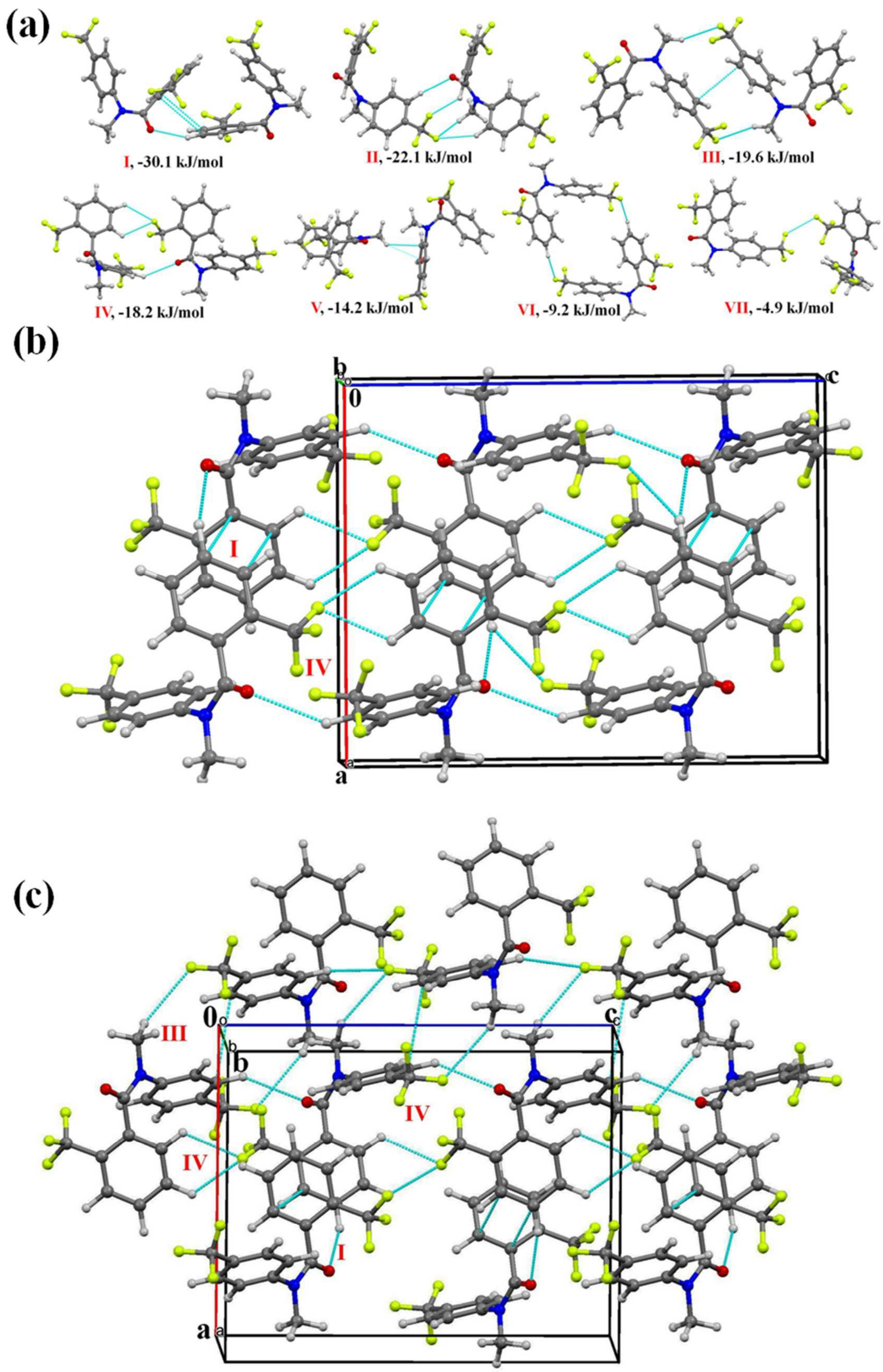
(a)
I, -30.1 kJ/mol
II, -22.1 kJ/mol
III, -19.6 kJ/mol
IV, -18.2 kJ/mol
V, -14.2 kJ/mol
VI, -9.2 kJ/mol
VII, -4.9 kJ/mol
(b)
I
IV
(c)
III
IV
IV
I

Figure 11(a): Molecular pairs extracted from crystal packing of **NM31** along with their interaction energies. **(b)** Packing of molecules down the *ab* plane in **NM31** *via* weak C(sp^2)-H···O=C, C-H···F-C(sp^3) hydrogen bonds and π···π interactions. **(c)** Packing of molecules down the *ac* plane with the utilization of weak C(sp^2)-H···O=C, C-H···F-C(sp^3) hydrogen bonds and π···π interactions in **NM31**.

***N*-methyl-4-(trifluoromethyl)-*N*-(4-(trifluoromethyl)phenyl)benzamide (NM33):**

The compound **NM33** crystallizes in the centrosymmetric triclinic space group *P*-1 with Z = 4 (Z′= 2). Selected molecular motifs, which contribute towards the stabilization of the crystal packing, are presented in **Figure 12(a)**. The two molecules in the asymmetric unit was observed to be connected *via* motif **IV** (I.E = -28.2 kJ/mol) which involves the presence of a bifurcated, short and directional C(sp^2)-H···O=C (2.30Å, 169°; 2.42Å, 136°) hydrogen bond, the stabilization energy having a substantial electrostatic contribution of 59% (**Table 5**). There are three more stabilized molecular pairs (motif **I**, **II**, **III**) than motif **IV** which were recognized in the crystal packing. The arrangement of the first four molecular motifs in the crystal packing of **NM33** has been depicted in **Figure 12(b)** down the crystallographic *bc* plane. The highest stabilized molecular motif **I** (I.E = -37.8 kJ/mol; %E_{elec} being 40%) consists of short and highly directional dimeric C(sp^2)-H···O=C (2.49Å, 173°) hydrogen bond. The stabilization of the motif **I** is significantly high than motif **IV**, although both possess similar interactions. The reason for this may be the presence of some long range dispersion interactions in motif **I**, as the net contribution from the dispersion energy in motif **I** were observed to be almost double than that in motif **IV** (**Table 5**). In motif **II** (I.E = -35.3 kJ/mol), the molecules were found to be linked *via* weak C-H···π and π···π, the contribution from dispersion being significantly high (75%) while three weak C(sp^2)-H···F-C(sp^3) hydrogen bonds along with π···π interactions were recognized to link the molecules in motif **III** with %E_{disp} contribution being reduced to 66%. Furthermore, motif **V** (I.E = -21.9 kJ/mol) and **VI** (I.E = -21.9 kJ/mol) were observed to provide similar stabilization to the crystal packing but the involved interactions were recognized to be significantly different. A weak C(sp^3)-H···O=C hydrogen bond along with a short C(sp^3)-H···π (2.63Å, 138°) and π···π interactions were found to stabilize motif **V** whilst it is mainly the latter which linked the molecules in motif **VI**. The differences associated in the nature of interactions in the two motifs **V** and **VI** is clearly reflected in the dispersion energy contribution, as it is 67% in case of former while 78% in case of the latter. A very short C(sp^2)-H···O=C (2.20Å, 148°) hydrogen bond, involving acidic hydrogen, along with a weak C(sp^3)-H···F at higher distance

(2.81Å, 125°) were observed to stabilize the crystal packing (motif **VII**, I.E = -15.0 kJ/mol) having a substantial electrostatic contribution (65%). A weak C(sp^3)-F···C=O interaction and C(sp^3)-H···F hydrogen bond (motif **VIII**, I.E is -14.0 kJ/mol) were found to direct the molecular chain of molecule 2 along the crystallographic *a*-axis [**Fig. 12(c)**]. Such chains were observed to be linked with adjacent molecular chains, formed with utilization of weak bifurcated C(sp^2) /(sp^3)-H···F hydrogen bond along the *a*-axis (motif **IX** ; I.E = -10 kJ/mol), *via* the presence of different intermolecular interactions involved in motifs **II**, **IV**, **V** and **VII** [**Fig. 12(c)**].

It is to be mentioned that weakly stabilized molecular motifs possessing interactions involving organic fluorine were recognized in the crystal packing of **NM33** with the stabilization energies in the range of 10 kJ/mol to 1.2 kJ/mol [motif **IX – XIV, Fig. 12(a)**]. The motifs **IX**, **X** and **XI** were observed to provide similar stabilization (-10kJ/mol) but involve interactions of different nature and geometry. The motif **IX** was found to involve bifurcated C(sp^2)/(sp^3)-H···F hydrogen bond (with one at short distance; 2.43Å, 148°) while a dimeric C(sp^2)-H···F and C(sp^3)-F···F-C(sp^3) were observed in motif **X**. Further, in case of motif **XI**, a bifurcated C(sp^3)-H···F hydrogen bond (with one being short and directional; 2.48Å, 160°) was recognized. Unlike motif **IX**, it involves a bifurcated acceptor wherein two fluorine atoms of one CF_3 group are involved in the formation of the hydrogen bond with a hydrogen atom of the CH_3 group. Moreover, the motifs, **XII** and **XIII** was observed to consist of weak C(sp^2)-H···F-C(sp^3) hydrogen bond, providing similar stabilization (8.0 and 7.2 kJ/mol respectively). A dimeric C(sp^3)-F···F-C(sp^3) interaction (with one contact , *Type I geometry*: 2.889(1)Å / 101(1)° / 101(1)°) were recognized in the formation of a molecular motif **XIV** [**Fig. 11(a)**], which provides the least stabilization (I.E = -1.2 kJ/mol) to the crystal packing. The partition of the interaction energy into different contributions indicates positive coulombic contribution, the net stabilization originating mainly from the dispersive contribution (96%, **Table 5**).

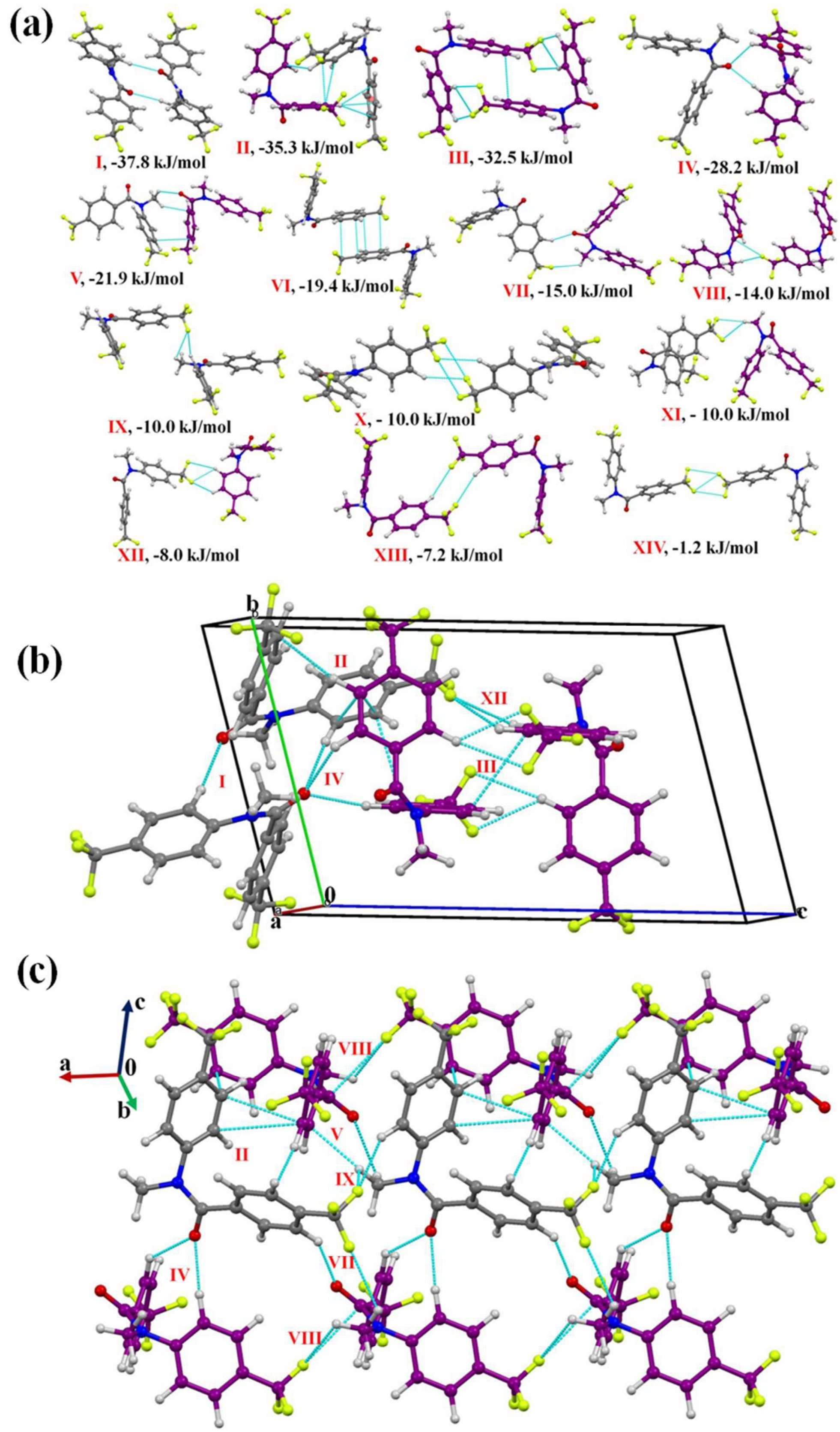
(a)
I, -37.8 kJ/mol
II, -35.3 kJ/mol
III, -32.5 kJ/mol
IV, -28.2 kJ/mol
V, -21.9 kJ/mol
VI, -19.4 kJ/mol
VII, -15.0 kJ/mol
VIII, -14.0 kJ/mol
IX, -10.0 kJ/mol
X, - 10.0 kJ/mol
XI, - 10.0 kJ/mol
XII, -8.0 kJ/mol
XIII, -7.2 kJ/mol
XIV, -1.2 kJ/mol
(b)
b
II
XII
III
I
IV
0
a
c
(c)
c
a
0
b
VIII
V
II
IX
VII
IV
VIII

Figure 12(a): Displaying selected molecular motifs connected with different intermolecular interactions in the crystal packing of **NM33. (b**) Part of the crystal packing down the *bc* plane in **NM33**, depicting presence of weak C(sp^2)-H···O=C, C-H···π and C(sp^2)-H···F-C(sp^3) hydrogen bonds along with π···π interactions. **(c)** Packing of molecules in **NM33** *via* the network of weak C-H···O=C, C-H···π and C-H···F-C(sp^3) hydrogen bonds along with π···π and C(sp^3)-F···C=O interactions.

Comparison of the crystal structures

From the analysis of the crystal structures of 11 compounds (ten derivatives of *N*-methyl-*N*-phenylbenzamide plus one unsubstituted compound) in this study, it was observed that seven molecules crystallized in the monoclinic space group $P2_1/c$ (including **NM03**, **NM30** with Z′ = 2 and **NM11**, where molecule prefers *trans* geometry) and none of them appeared to be isostructural [72]. This also includes compounds **NM10** and **NM00** which crystallized in the same space group, orthorhombic centrosymmetric *Pbca*. Furthermore, except **NM11**, all the compounds in this series appeared to have similar molecular conformation (*cis*-geometry) [**Fig. 1(c)**]. Hence it was of interest to compare these crystal structures to gain insights into the similarities and dissimilarities associated with the crystal packing. For this purpose XPac 2.0 [73-74] was used to analyze the crystal packing of these structures excluding **NM11**. The details of this analysis are presented in section S2 in ESI. XPac identified the similar packing arrangements in the two crystal structures, termed as 'supramolecular constructs (SC). It can be 3D (exactly similar arrangement or isostructural), 2D (layer of molecules are similar), 1D (a row of molecules similar) or 0D similarity (isolated unit like dimers are identical in the packing). The measure of the extent with which the two crystal structures deviate from the perfect geometrical similarity is defined as 'dissimilarity index (X)' [75]. Lower the value of X, better is the structural match. The analysis of the ten crystal structures (**Table S2**) revealed that the arrangement of the molecules match (the presence of 2D SC) in case of **NM02** (packing of molecule 1) and **NM03** (packing of molecule 2) with X = 6.7 (labeled as 'C1' **Fig. 13** & **S7, Table S2**). There was presence of 1D SCs [the presence of a molecular chain (6 types, B1 to B6), **Fig.13** & **S8, Table S2**] observed in case of pairs NM02_ 2/NM03_1; NM02_2/NM10; NM03_1/NM10; NM12/NM22; NM22/NM23; NM31/NM33_2. There were 6 different types (A1 to A6, **Fig. 13** & **S9**) of similar molecular dimers (presence of 0D SC) also recognized in the different pairs of the crystal structure (**Table S2**).

It was of further interest to compare all the present crystal structures with related crystal structures reported in the CSD [**Fig. 1(d)**]. Comparison of the structures having *cis*-geometry (CSD ref code: YEGJEY, YEGKEA, YEGKIE, YEGKOK and YEGLAX) revealed no similarity with the unsubstituted compound, NM00 (ref code: JAZJOJ10) [**Table S2**]. There was presence of a similar molecular chain (1D SCs) on comparison of NM03_1, NM10, NM12 with YEGLAX [**Fig. S10(a)**, **Table S2**] which is analogous with the chain 'B2' [in pair NM03_1/NM10; **Fig. S8(b)**]. In addition, the existence of 1D SC (similar chain) was also recognized for NM22/YEGLAX. Moreover, pairs NM03_1/YEGKEA, NM10/YEGKEA, NM10/YEGKOK, NM12/YEGKEA and NM23/YEGKEA display the presence of a similar molecular robust dimer (equivalent with the dimer 'A1'; 0D SCs) in their crystal packing [**Fig. S11(a)**]. Further, the presence of 0D SCs (similar molecular pairs) was also observed for pairs NM02_1/YEGKOK, NM02_1/YEGLAX NM22/YEGKOK, NM31/YEGLAX and NM22/YEGKOK [**Fig. S11(b – (d)**]. Furthermore, the comparison of the crystal structure of NM11 with the structure reported in the CSD with *trans* geometry (ref code: YEGJEY, DIBGIF and DIBGAX) indicates the presence of similar chains in case of pairs, NM11/ DIBGAX_1 and NM11/ DIBGAX_4 and surprisingly no similarity was observed for NM11/YEGJEY (having four methyl substitution at *ortho* positions of both the phenyl rings in the molecule). Hence from the overall comparison of crystal structures it can be observed that although none of these structures are isostructural, but the presence of similar structural motifs can be realized in their crystal packing.

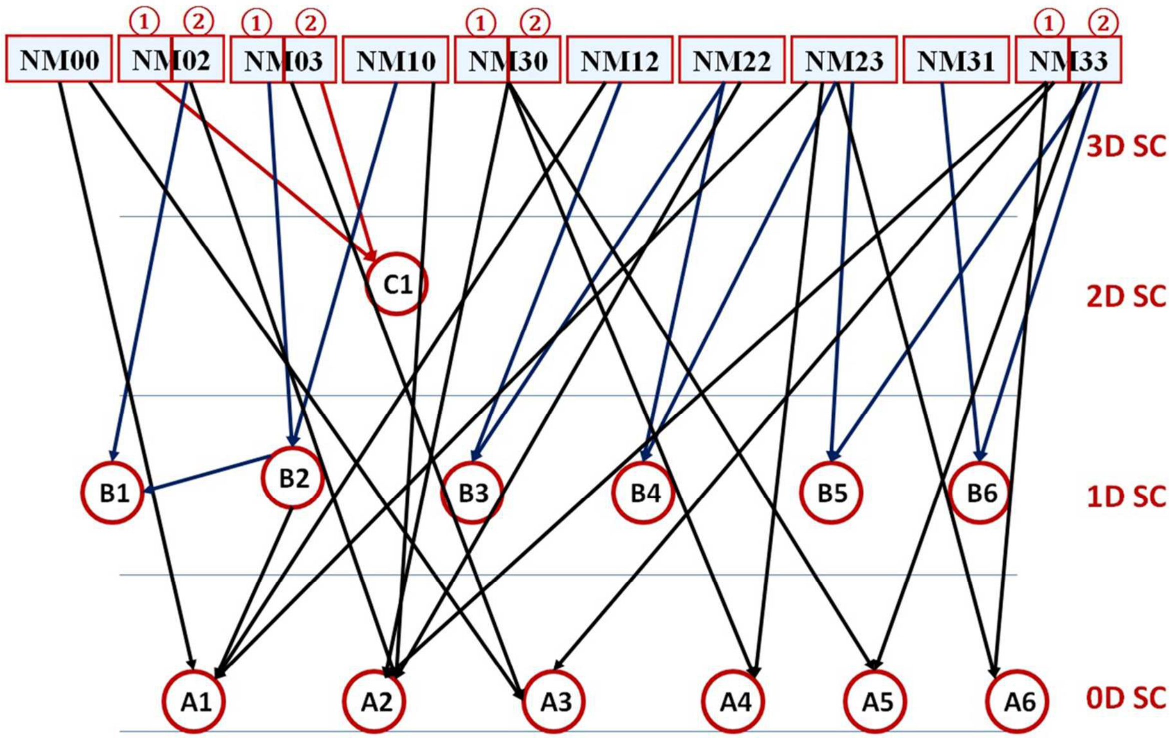

Figure 13: Relationship of all the crystal structures from XPac analysis (section S2, ESI). The compounds **NM02**, **NM03**, **NM30** and **NM33** have two symmetry independent molecules, represented by the number in circle.

Conclusions

The complete quantitative analysis of the molecular and crystal structure of ten out of the fifteen newly synthesized trifluoromethyl substituted *N*-methyl-*N*-phenylbenzamides reveals the significance of weak interactions in stabilizing the molecular and crystal structure in absence of any strong donor atom. Unlike the *N*-phenylbenzamides, the derivatives of *N*-methyl-*N*-phenylbenzamide prefer to possess *cis*-conformation, wherein the molecular structure is stabilized by the presence of weak C(sp^3)-H···O=C hydrogen bond. The steric crowd at the *ortho* position of both the phenyl rings may change the conformation to *trans* geometry similar to as observed in *N*-phenylbenzamide.

The computational procedures which involve calculation of the lattice energy and the evaluation of the interaction energies for different intermolecular interactions provide detailed insights into the nature of the weak intermolecular interactions present in the crystal packing of this series of compounds. In the absence of a strong donor, the crystal packing was observed to be stabilized by the cooperative interplay of the presence of weak intermolecular interactions like C-H···O=C, C-H···π hydrogen bond along with other weak interactions like π···π stacking. There are short C-H···O=C hydrogen bonds which were observed in the crystal packing of these compounds with substantially high electrostatic (coulombic + polarization) contribution. The interactions involving organic fluorine namely C-H···F-C, C-F···F-C, C-F···F-C are ubiquitous and does provide stabilization, albeit less, to the crystal packing and are observed to involve in the formation of different unique structural motifs. The detailed and comparative analysis of the nature of different interactions which are involved in the different molecular motifs in the crystal packing with detailed inputs from energy calculations, using the PIXEL method brings out the following observations: (i) the interaction energy in the decreasing order of weak hydrogen bonds as follow: C-H···O=C > C-H···π > C-H···F-C (ii) The contribution from dispersion energy towards the total stabilization follows the order: C-H···O=C < C-H···F-C < C-H···π (contribution from electrostatic follows opposite order) (iii) There is an increase in the electrostatic contribution observed at short distance and directional hydrogen bonds present in the molecular motif. In futuristic studies, it is of interest to extend this study of investigation of interactions involving organic fluorine in different electronic and chemical environments.

Acknowledgements

PP thanks UGC-India for research scholarship. We acknowledge IISER Bhopal for research facilities and infrastructure. The authors also thank Prof T. N. Guru Row for SCXRD and PXRD data collection on the CCD facility at IISc, Bangalore under the IRHPA-DST Scheme. DC thanks DST-Fast Track Scheme for research funding.

References:

1. G. R. Desiraju, *J. Am. Chem. Soc*. 2013, **135**, 9952 - 9967.

2. H.-J. Schneider, *Angew. Chem. Int. Ed.* 2009, **48**, 3924-3977.

3. J. D. Dunitz and Gavezzotti, A. *Chem. Soc. Rev*. 2009, **38**, 2622 - 2633.

4. A. Nangia and G. R. Desiraju, in *Design of Organic Solids*, ed. E. Weber, Springer-Verlag, Berlin, 1998.

5. D. Philip, and J. F. Stoddart, *Angew. Chem., Int. Ed*. 1996, **35***,* 1154−1196.

6. P. Panini, K. N. Venugopala, B. Odhav and D. Chopra, *Acta Cryst.* 2014, **B70**, 681–696.

7. E. Arunan, G. R. Desiraju, R. A. Klein, J. Sadlej, S. Scheiner, I. Alkorta, D. C. Clary, R. H. Crabtree, J. J. Dannenberg, P. Hobza, H. G. Kjaeergaard, A. C. Legon, B. Mennucci and D. J. Nesbitt, *Pure Appl. Chem.*, 2011, **83**, 1619-1636.

8. G. R. Desiraju and T. Steiner, *The Weak Hydrogen Bond in Structural Chemistry and Biology*, Oxford University Press: Oxford, 1999.

9. C.A. Hunter, *Angew. Chem. Int. Ed*. 2004, **43**, 5310 – 5324.

10. O. Takahashi, Y. Kohno and M. Nishio, *Chem. Rev*. 2010, **110**, 6049-6076.

11. M. Nishio, *Phys. Chem. Chem. Phys*. 2011, **13**, 13873-13900.

12. (a) K. Reichenbacher, H. I. Suss and J. Hulliger, *Chem. Soc. Rev.*, 2005, **34**, 22. (b) P. Panini and D. Chopra, In *Hydrogen Bonded Supramolecular Structures*, Eds. Z. Li and L. Wu, *Lecture Notes in Chemistry,* 2015, **87**, 37 -67. Springer-Verlag, Berlin, Heidelberg

13. (a) H. -J. Schneider, *Chem. Sci.,* 2012, **3**, 1381- 1394. (b) R. Shukla and D. Chopra, *CrystEngComm*, 2015, **17**, 3596-3609.

14. M. Egli, *Acc. Chem. Res.* 2012, **45**, 1237 - 1246.

15. D. O'Hagan, *Chem. Soc. Rev.* 2008, 37, 308-319.

16. B. E. Smart, *J. Fluorine. Chem.* 2001, **109**, 3-11.

17. H. J. Bohm, D. Banner, S. Bendels, M. Kansy, B. Kuhn., K. Muller, U. Obst-Sander and M. Stahl., *ChemBioChem,* 2004, **5**, 637 - 643.

18. J. Wang., M. Sanchez-Rosello., J. L. Acena., C. D. Pozo., A. E. Sorochinsky, S. Fustero, V. A. Soloshonok. and H. Liu, *Chem. Rev.*, 2014, **114**, 2432 – 2506.

19. J. D. Dunitz, *ChemBioChem***,** 2004, **5**, 614−621.

20. P. Panini and D. Chopra, *CrystEngComm*, 2013, **15**, 3711–3733.

21. (a) P. Panini and D. Chopra, *CrystEngComm,* 2012, **14**, 1972−1989. (b) P. Panini and D. Chopra, *Cryst. Growth Des.* 2014, **14**, 3155−3168.

22. M. Perez-Torralba, M. A.García, C. Lopez, M. C. Torralba, M. R. Torres, R. M. Claramunt and J. Elguer, *Cryst Growth Des,* 2014, **14**, 3499–3509.

23. S. Terada, K. Katagiri, H. Masu, H. Danjo, Y. Sei, M. Kawahata, M. Tominaga, K. Yamaguchi and I. Azumaya, *Cryst Growth Des.*, 2012, **12**, 2908 - 2916.

24. A. Abad, C. Agulló, A. C. Cuñat, C. Vilanova, de. Ramírez and M. C. Arellano, *Cryst. Growth Des*., 2006, **6**, 46 - 57.

25. K. Müller, C. Faeh and F. Diederich, *Science*, 2007, **317**, 1881.

26. R. Berger, G. Resnati, P. Metrangolo, E. Weber and J. Hulliger, *Chem. Soc. Rev*. 2011, **40**, 3496−3508.

27. D. Chopra, *Cryst.Growth Des.* 2012, **12**, 541 - 546.

28. D. Chopra and T. N. Guru Row, *CrystEngComm.* 2011, **13**, 2175−2186.

29. A. R. Choudhury and T. N. Guru Row, *Cryst. Growth Des.* 2004, **4**, 47−52.

30. D. Chopra and T. N. Guru Row, *CrystEngComm*, 2008, **10**, 54−67.

31. G.. Kaur and A. R. Choudhury, *Cryst. Growth Des.* 2014, **14**, 1600–1616.

32. G. Kaur, P. Panini, D. Chopra and A. R. Choudhury, *Cryst Growth Des*., 2012. **12**, 5096 - 5110.

33. M. Karanam and A. R. Choudhury, *Cryst. Growth Des.* 2012, **13**, 4803.

34. V. Vasylyeva and K. Merz, *Cryst. Growth Des*. 2010, **10**, 4250−4255.

35. A. G. Dikundwar, R. Sathishkumar, T. N. Guru Row, G. R. Desiraju, *Cryst. Growth. Des.* 2011, **11**, 3954−3963.

36. V. R. Hathwar, D. Chopra, P. Panini and T. N. Guru Row, *Cryst. Growth. Des.* 2014, *14*, 5366–5369.

37. O. Jeannin and M. Fourmigue, *Chem.–Eur. J.* 2006, **12**, 2994 - 3005.

38. C. Jackel, M. Salwiczek and B. Koksch, *Angew. Chem., Int. Ed.*, 2006, **45**, 4198 - 4203.

39. M. Fioroni, K. Burger, A. E. Mark and D. Roccatano, *J. Phys. Chem. B*, 2003, **107**, 4855 - 4861.

40. J. L.Kgokong, P. P. Smith and G. M. Matsabisa, *Bioorg. Med. Chem.* 2005, **13**, 2935-2942.

41. J. A. K. Howard and H. A. Sparkes, *CrystEngComm*, 2008, **10**, 502 - 506.

42. (a) D. E. Braun, T. Gelbrich, V. Kahlenberg, G. Laus, J. Wieser and U. J. Griesser, *New J. Chem.*, 2008, **32**, 1677 – 1685 (b) M. O. BaniKhaled, J. D. Mottishaw and H. Sun, *Cryst. Growth Des*., 2015, **15**, 2235−2242.

43. I. Azumaya, K. Yamaguchi, H. Kagechika, S. Saito, A. Itai and K. Shudo, *Pharma. Soc. Japan*, 1994, **114**, 414-430.

44. I. Azumaya, H. Kagechika, K.Yamaguchi and K. Shudo, *Tetrahedron*, 1995, **51**, 5277- 5290.

45. R. Yamasaki, A. Tanatani, I. Azumaya, H. Masu, K. Yamaguchi and H. Kagechika, *Cryst. Growth Des.* 2006, **6**, 2007-2010.

46. I. Azumaya, H. Kagechika, Y. Fujiwara, M. Itoh, K. Yamaguchi and K. Shudo, *J. Am. Chem. Soc.* 1991, **113**, 2833 – 2838.

47. F. D. Lewis and W. Liu, *J. Phys. Chem. A*, 2002, **106**, 1976 – 1984.

48. T. Hirano, T. Osaki, S. Fujii, D. Komatsu, I. Azumaya, A. Tanatani and H. Kagechika, *Tetrahedron Lett.* 2009, **50**, 488 – 491.

49. (a) L. Maschio, B. Civalleri, P. Ugliengo and A. Gavezzotti, *J. Phys. Chem.* A, 2011, 115, 11179 – 11186. (b)A. Gavezzotti, *New. J. Chem.* 2011, **35**, 1360 -1368.

50. (a) J. D. Dunitz and A. Gavezzotti, *Cryst. Growth Des.* 2005, **5**, 2180−2189. (b) P. Panini, K. N. Venugopala, B. Odhav and D. Chopra, *Acta Cryst.*, CrystEngComm Page 28 of 29 2014, B70, 681–696.

51. J. D. Dunitz and A. Gavezzotti, *Cryst. Growth Des.* 2012, **12**, 5873−5877.

52. A.Altomare, G.Cascarano, C. Giacovazzo, A. Guagliardi, *J.Appl.Crystallogr.*, 1993, **26**, 343−350.

53. L. J. Farrugia, *J. Appl. Cryst.* 2012, **45**, 849-854.

54. G. M. Sheldrick, *Acta Cryst*. 2008, **A64**, 112–122.

55. C. F. Macrae, I. J. Bruno, J. A. Chisholm, P. R. Edgington, P. McCabe, E. Pidcock, L. Rodriguez-Monge, R. Taylor, J. van de Streek, P. A. Wood, *J. Appl. Cryst.* 2008, **41**, 466–470.

56. M. Nardelli, *J. Appl. Cryst.* 1995, **28**, 659.

57. A. L. Spek, *Acta Cryst.* 2009, **D65**, 148–155.

58. TURBOMOLE V6.2 2010, a development of University of Karlsruhe and Forschungszentrum Karlsruhe GmbH, 1989-2007, TURBOMOLE GmbH, since 2007; available from http://www.turbomole.com.

59. M. J. Frisch, *et al*. *GAUSSIAN09, Revision A. 02.* Gaussian, Inc., Wallingford, CT, USA, 2009.

60. S. Grimme, J. Antony, S. Ehrlich and H. Krieg, *Chem. Phys.* 2010, **132**, 154104.

61. W. Hujo and S. Grimme, *Phys. Chem. Chem. Phys.* 2011, **13**, 13942–13950.

62. S. Grimme, *J. Comput. Chem.* 2006, **27**, 1787–1799.

63. R. Ahlrichs, M. Bar, M. Haser, H. Horn and C. Kolmel, *Chem. Phys. Lett.* 1989, **162,** 165–169.

64. S. F. Boys and F. Bernardi, *Mol. Phys.* 1970, **19**, 553 – 566.

65. S. L Cockroft, J. Perkin, C. Zonta, H. Adams, S. E. Spey, C. M. R. Low, J. G. Vinter, K. R. Lawson, C. J. Urch and C. A. Hunter, *Org. Biomol.Chem.* 2007, **5**, 1062 – 1080.

66. A. Bondi, *J. Phys. Chem.* 1964, **68**, 441−451.

67. A. Mukherjee and G. R. Desiraju, *IUCrJ*, 2014, **1**, 49 - 60.

68. P. Metrangolo and G. Resnati, *IUCrJ*, 2014, **1**, 5 - 7.

69. E. D'Oria and J. J. Novoa, *CrystEngComm.* 2008, **10**, 423-436.

70. S. Kawahara, S.Tsuzuki and T. Uchimaru, *J. Phys. Chem A*, 2004, **108**, 6744 – 6749.

71. R. M. Osuna, V. Hernẳndez, J. T. L. Navarrete, E. D'Oria and J. J. Novoa, *Theor Chem Acc.* 2011, 128, 541–553.

72. A. Kẳlmẳn, L. Pẳrnkẳnyi and G. Argay, *Acta Cryst.* 1993, **B49**, 1039-1049.

73. T. Gelbrich and M. B. Hursthouse, *CrystEngComm.* 2005, **7**, 324−336.

74. T. Gelbrich and M. B. Hursthouse, *CrystEngComm.* 2006, **8**, 448−460.

75. T. Gelbrich, T. L.Threlfall and M. B. Hursthouse, *CrystEngComm.* 2012, **14**, 5454−5464.

Table of Contents are as follows:

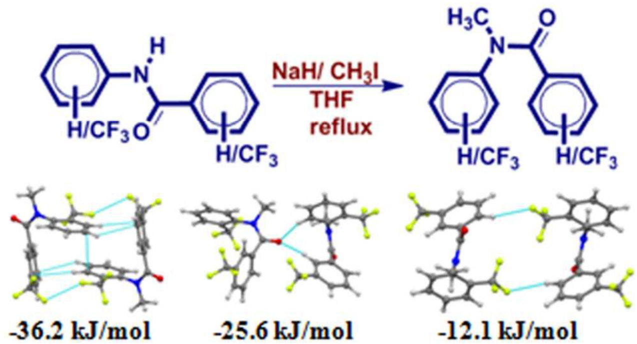

The nature and role of weak interactions involving fluorine in crystalline N-methyl-N-phenylbenzamides have been studied in the absence of strong H-bonds.